Rupture risk assessment of thoracic aortic aneurisms using advanced experimental and computational mechanics

MINES Saint-Étienne

SAINBIOSE
SAnté INgéniérie BIOlogie Saint-Etienne
U1059 • INSERM • SAINT-ETIENNE

Inserm
Institut national de la santé et de la recherche médicale

UNIVERSITÉ DE LYON

CHU Saint-Étienne

Prof. Stéphane AVRIL

MINES SAINT-ETIENNE
First Grande Ecole
outside Paris
Founded in 1816

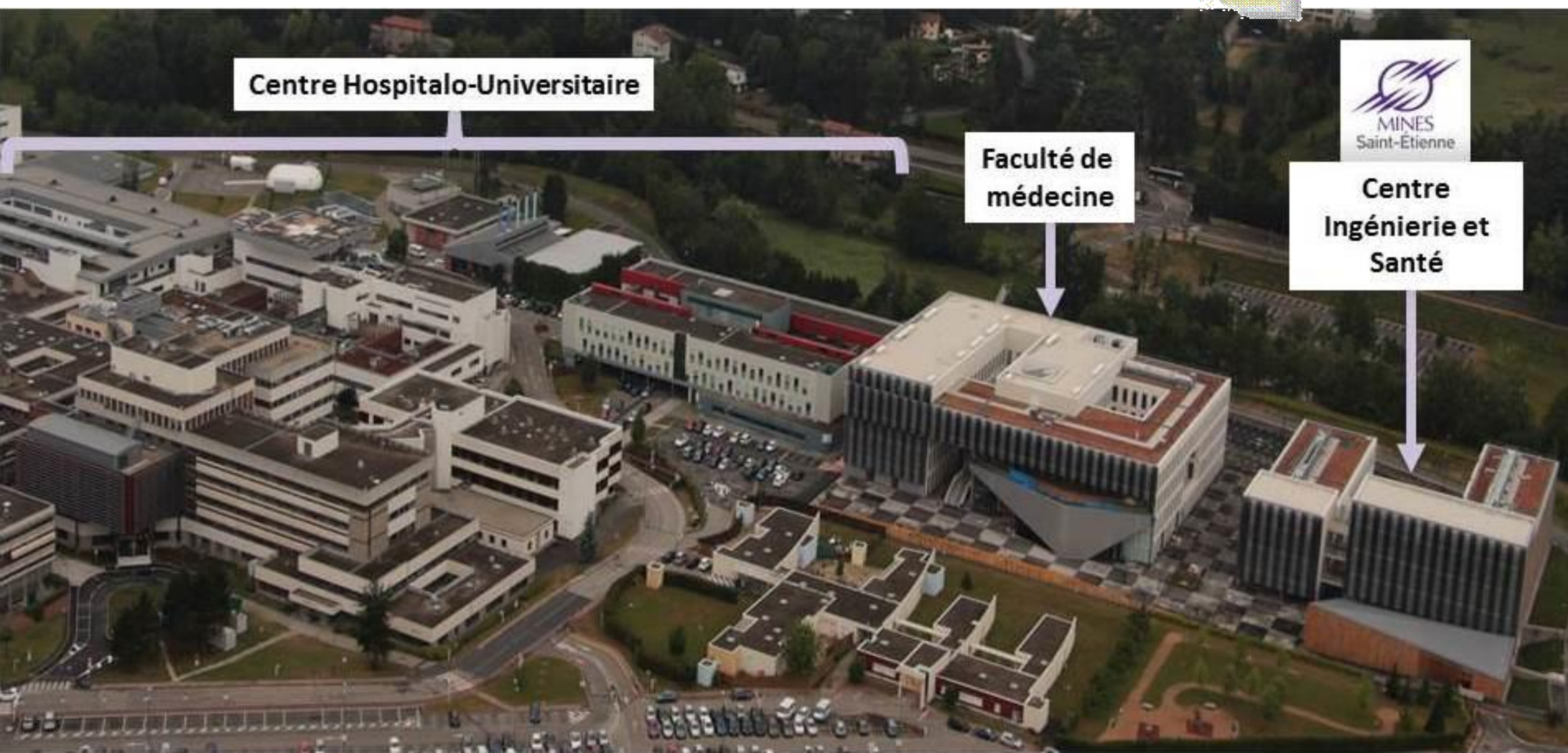

Computational mechanics in the OR for vascular surgery?

www.predisurge.com

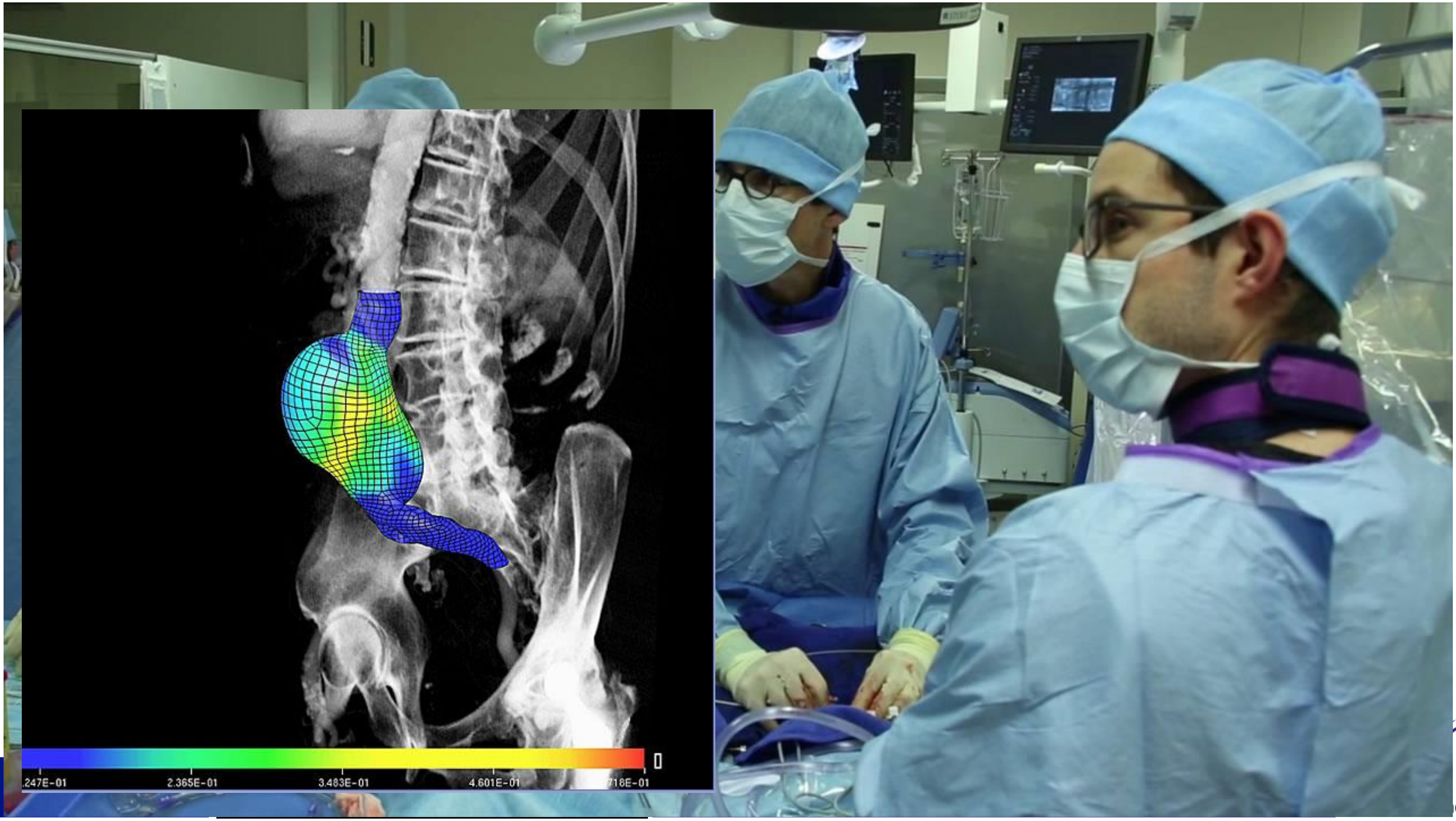

Arterial biomechanics and mechanobiology – Introduction

avril@emse.fr

Schematic representation of aortic structure

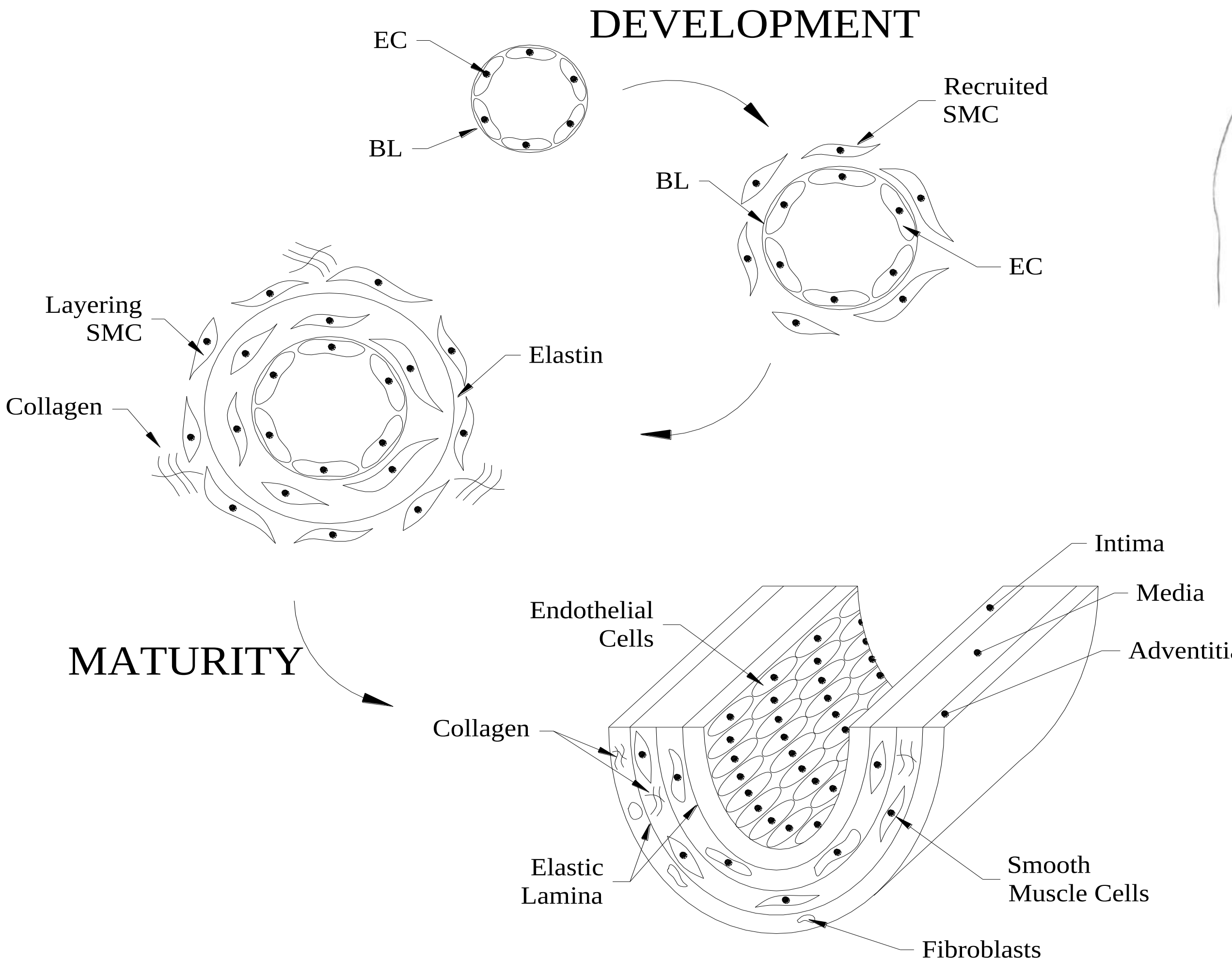

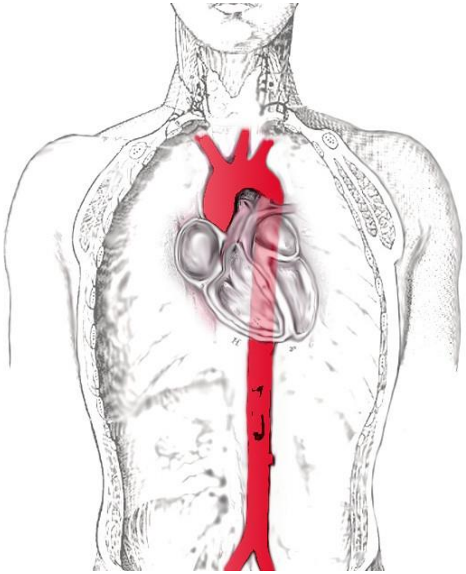

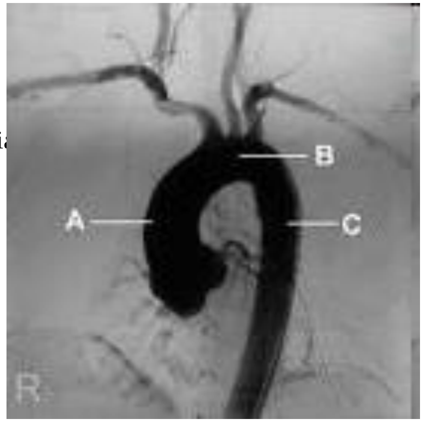

Functional biomechanical behavior

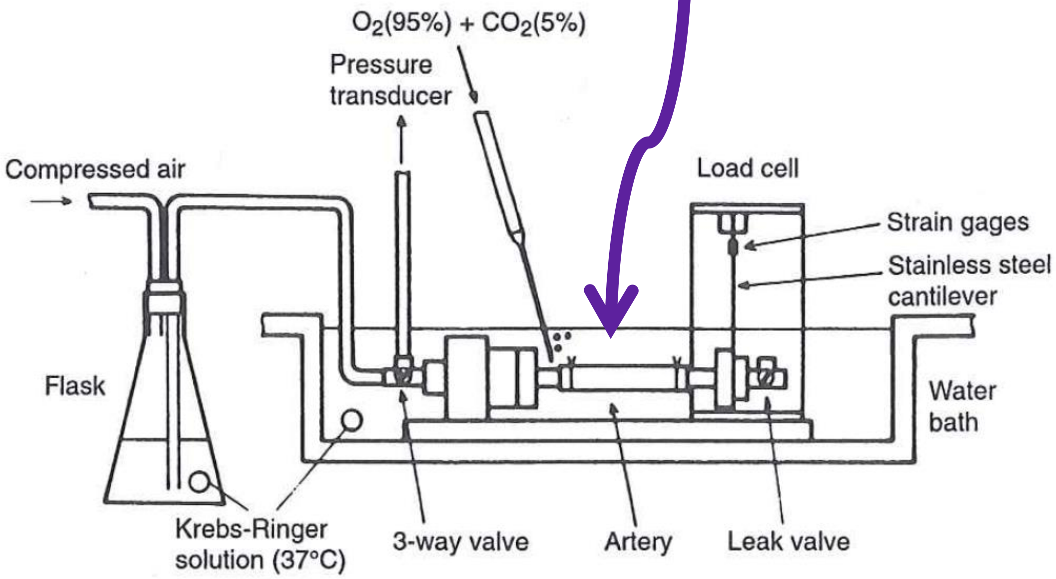

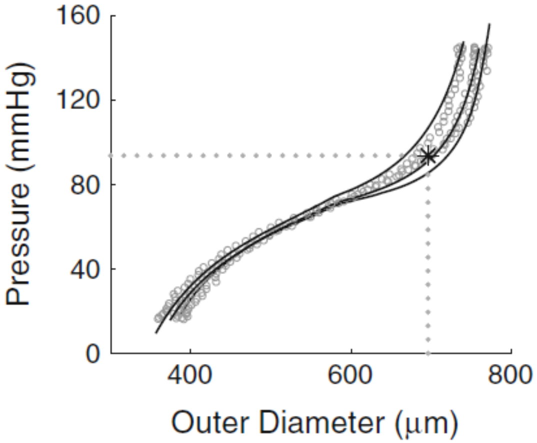

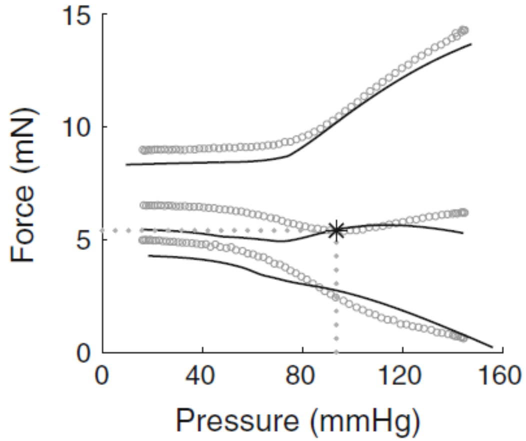

avril@emse.fr

MINES Saint-Étienne

Material characterization and constitutive modeling

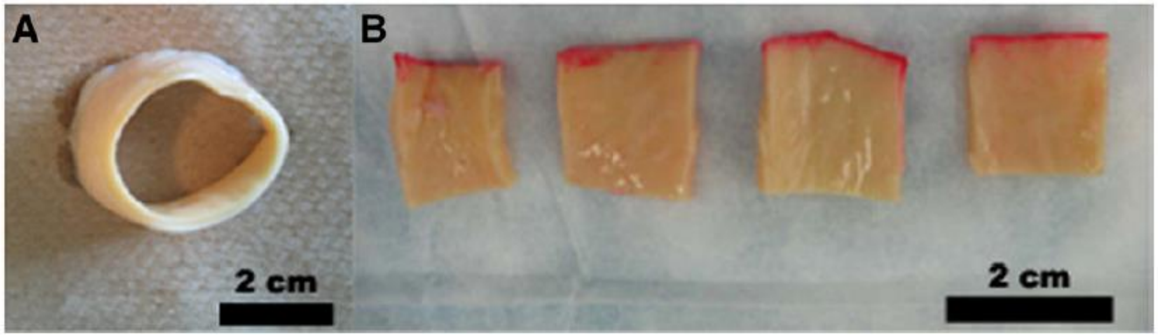

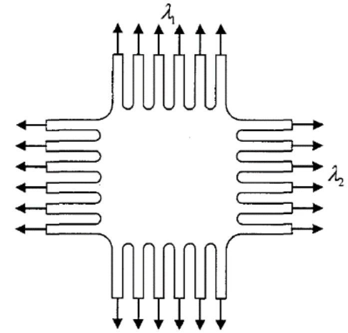

$$W = C_{10}\left(\overline{I}_1 - 3\right) + \frac{1}{D}\left(\frac{J^2 - 1}{2} - \ln J\right) + \frac{k_1}{2k_2}\sum_{\alpha=1}^{N}\left\{\exp\left[k_2\left\langle \overline{E}_\alpha\right\rangle^2\right] - 1\right\}$$

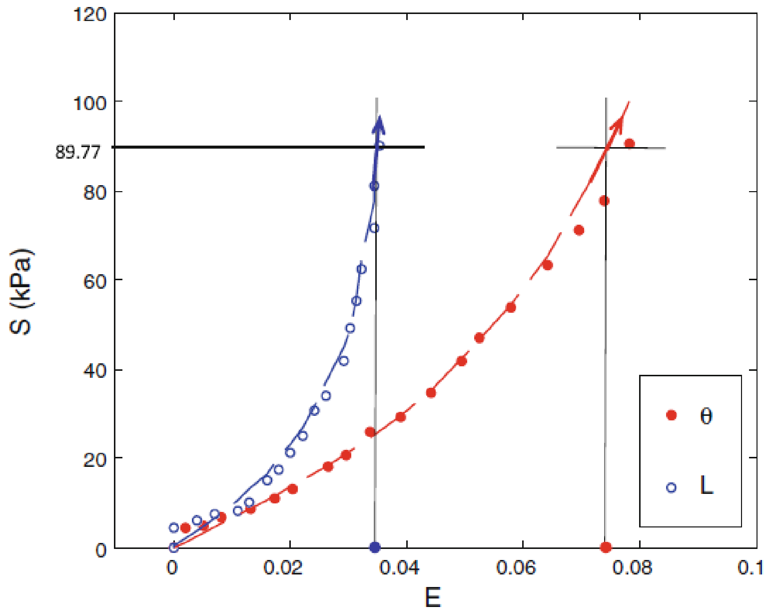

MEASUREMENT OF THE RESPONSE USING DIGITAL IMAGE CORRELATION

classical

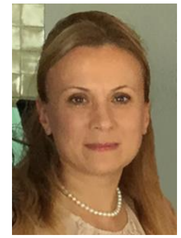

panoramic

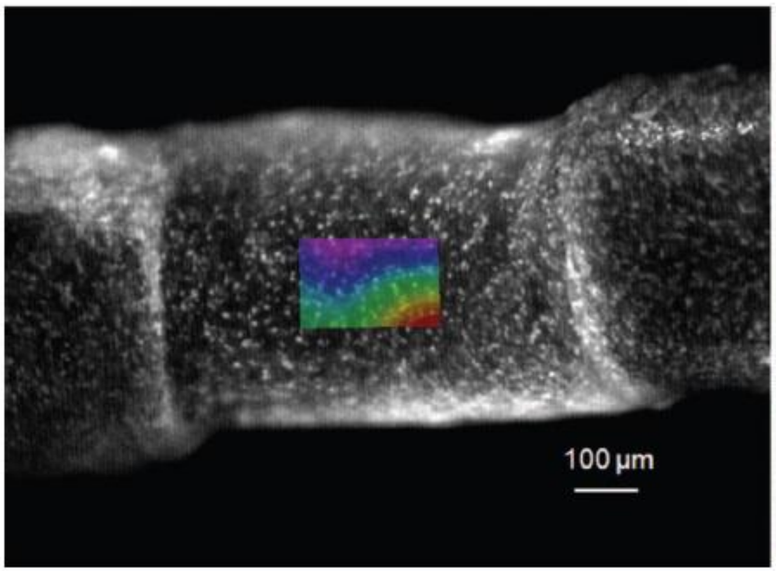

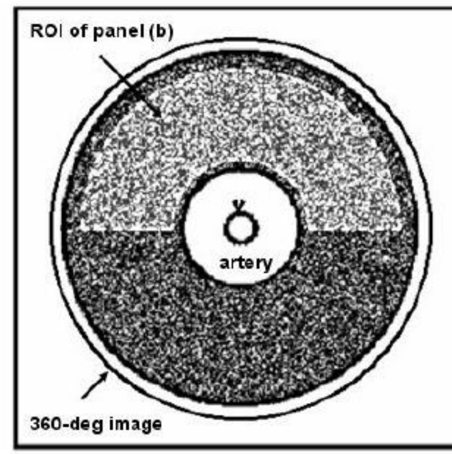

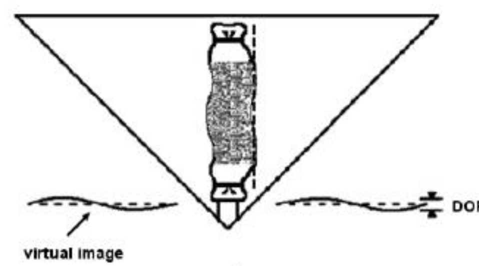

Badel et al. CMBBE, **15**, p 37-48, 2012.

Genovese. Optics Lasers Eng, **47**, p 995-1008, 2009.

Bulge inflation test

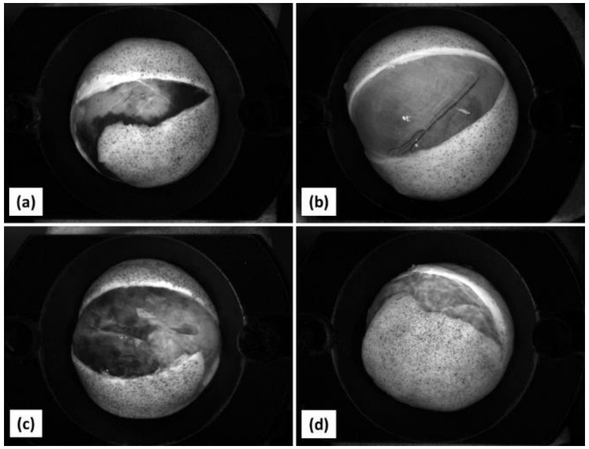

Romo et al. Journal of Biomechanics -2014

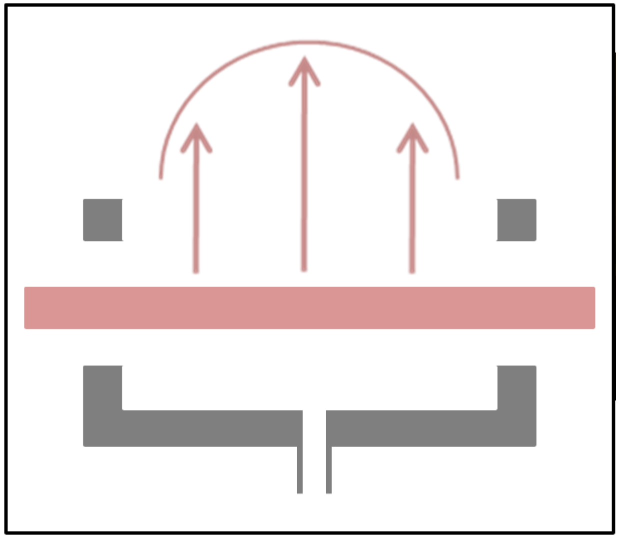

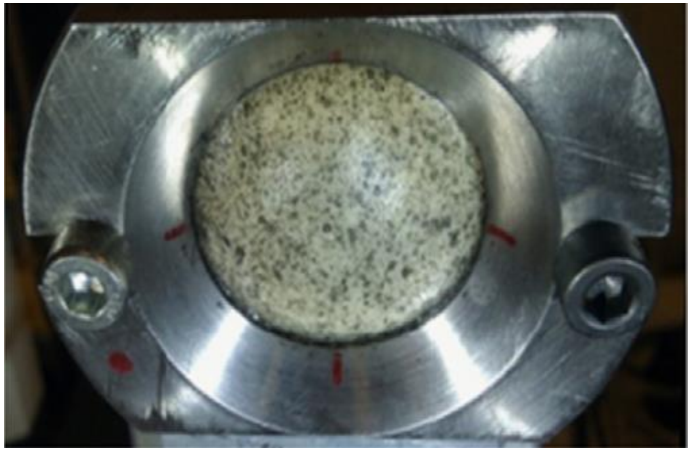

avril@emse.fr

Identification of local material properties

Davis et al. BMMB – 2015.
Davis et al. JMBBM – 2016
Zhao et al. Acta Biomaterialia - 2016

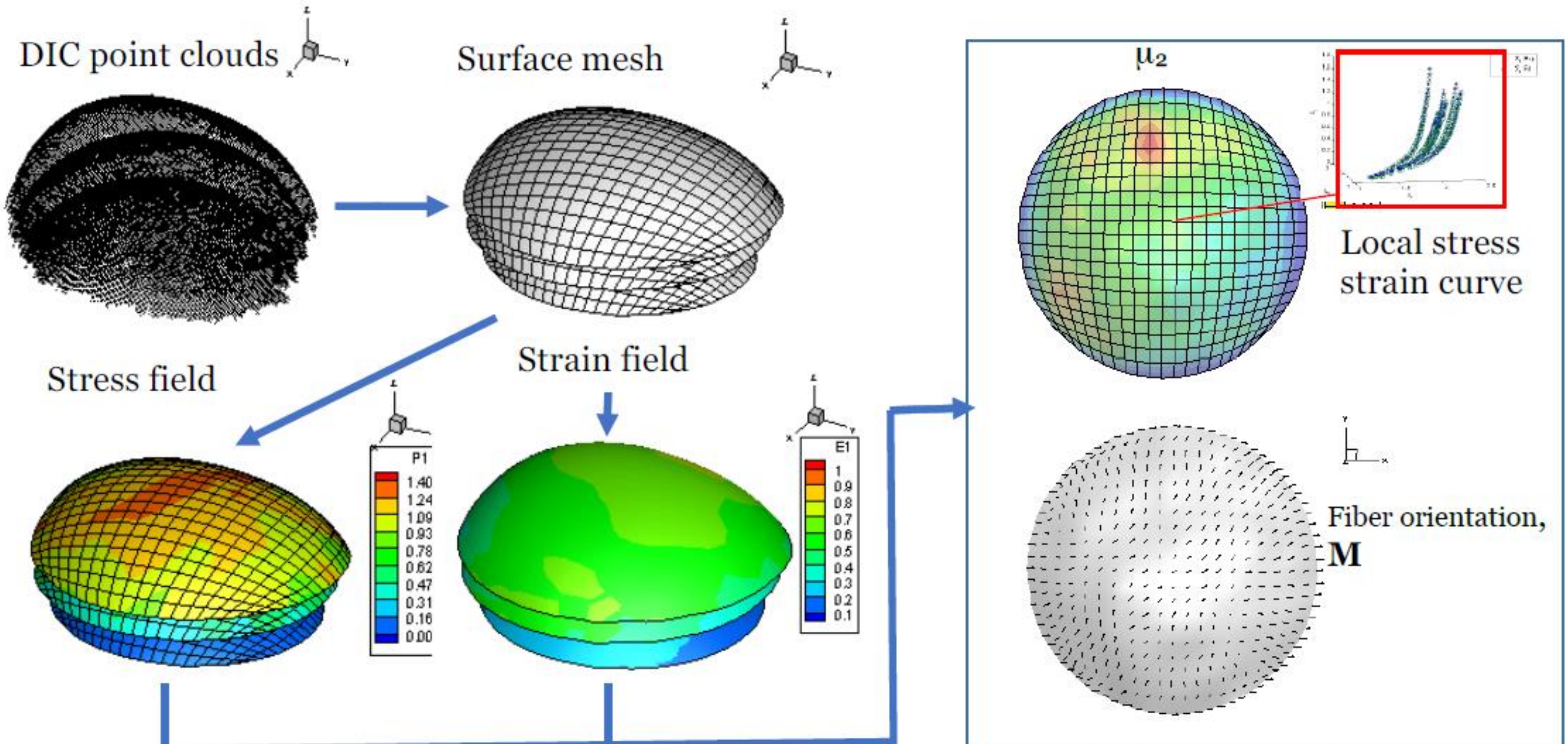

avril@emse.fr

Understanding aneurysm growth using mechanobiology and photomechanics

avril@emse.fr

Prediction of risk of rupture and dissection

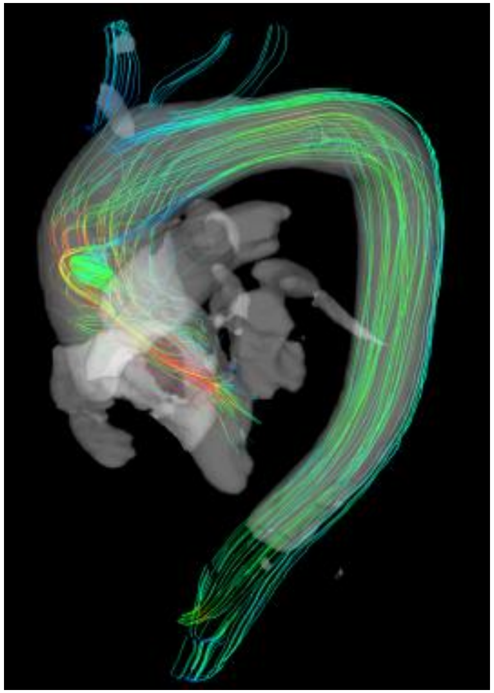

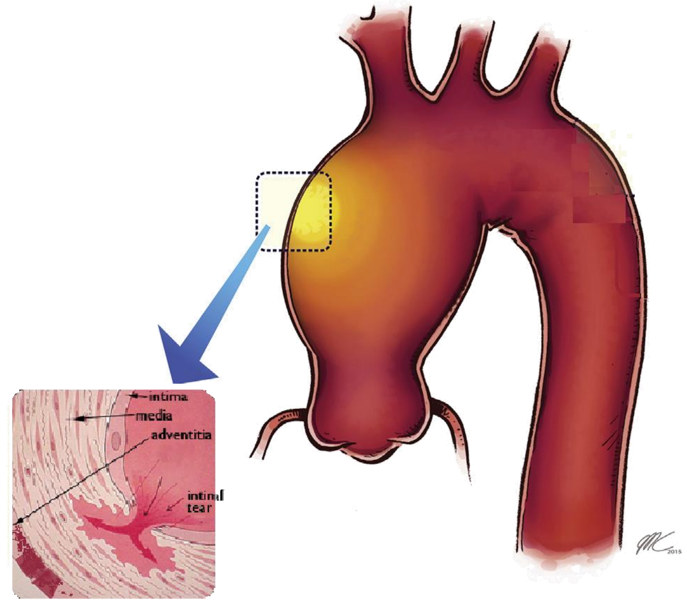

dissection

avril@emse.fr

Context

- **More and more aneurysms are detected at an early stage (incidence >8% for males >65 years old).**

- **An intervention is recommended if the aneurysm grows more >1cm/year or it is >5.5cm. This represents >90000 interventions per year in Europe and USA**

- **BUT:**
  - 25% aneurysms <5.5cm rupture : 15000 deaths**!
  - 60% of aneurysms >5.5 cm never experience rupture!

- **In summary: very high rate of inappropriate decisions and misprogramed surgical interventions!!**

** Pape et al, *Aortic Diameter ≥5.5 cm Is Not a Good Predictor of Type A Aortic Dissection Observations From the International Registry of Acute Aortic Dissection (IRAD)*, Circulation, 2007

TOWARDS ATAA GROWTH PREDICTIONS

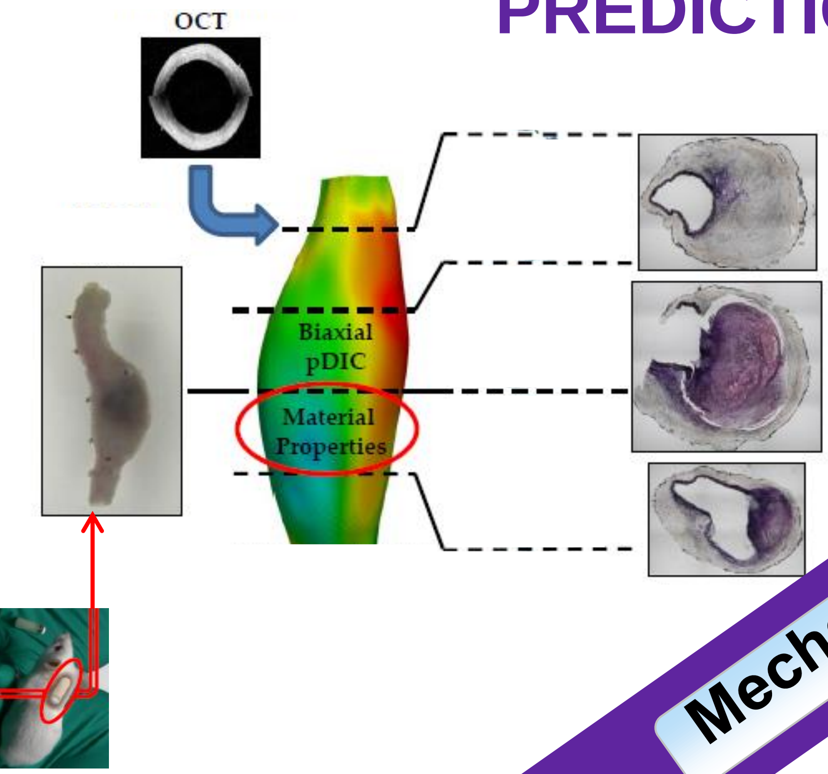

Clinical applications

Mechanobiology

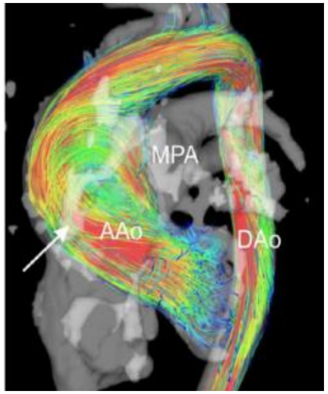

Development of mechanobiological models

avril@emse.fr

Altered mechanics induce biological responses, including gene expression, protein activation and cell phenotype

avril@emse.fr

APPROACH

1. **Experiments**
2. Material model
3. Inverse method

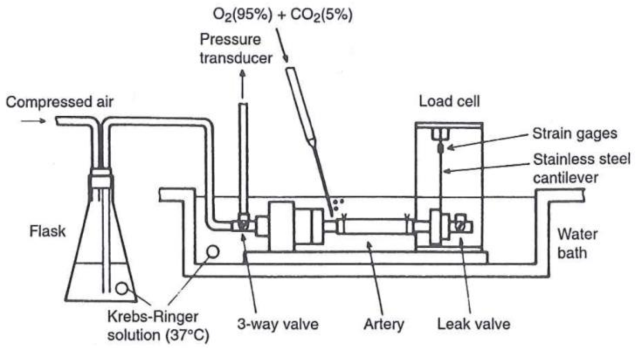

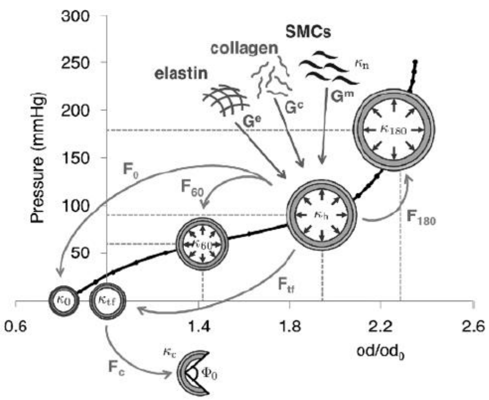

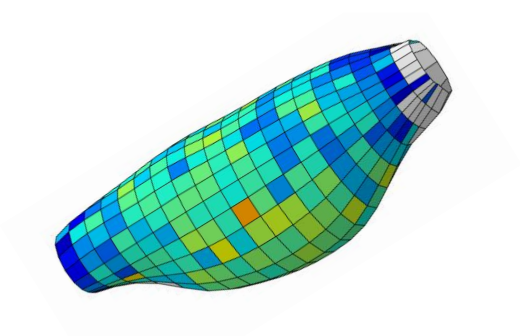

avril@emse.fr

MINES Saint-Étienne

Study Design

Control

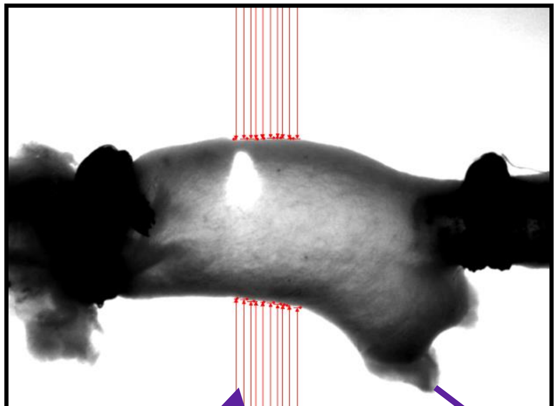

Fibulin 4 SMC KO

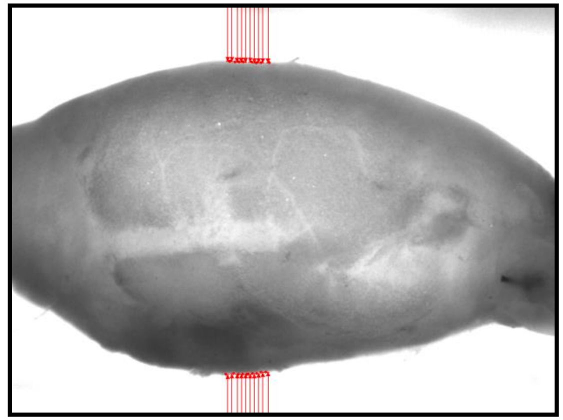

Fibrillin 1 *mgR/mgR*

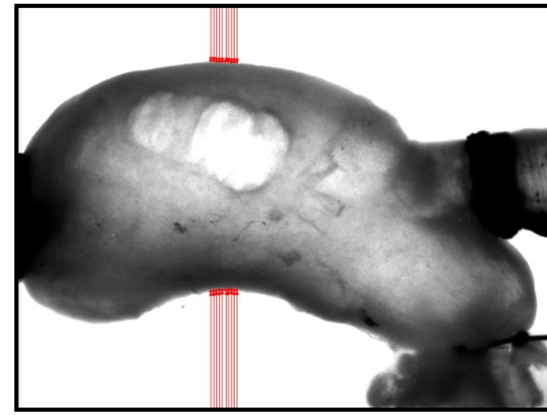

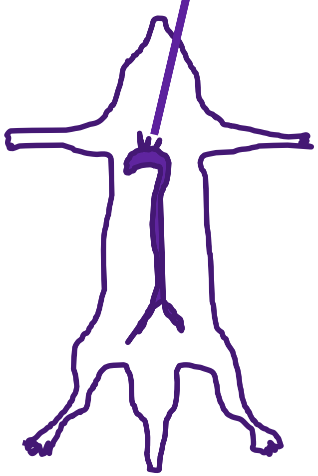

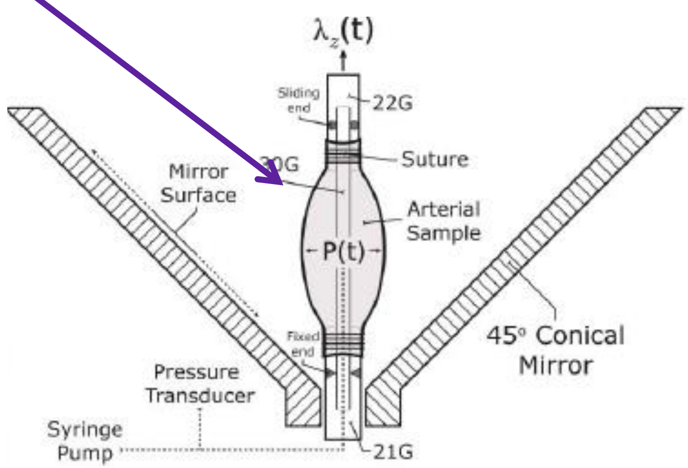

MINES Saint-Étienne

The pDIC technique

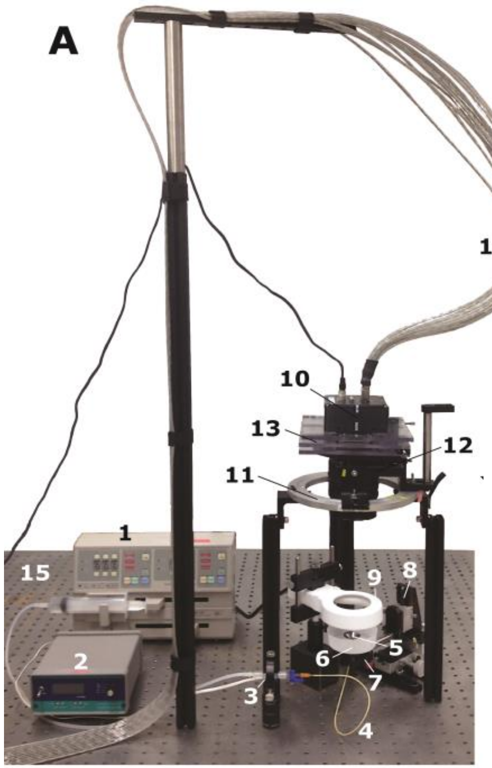

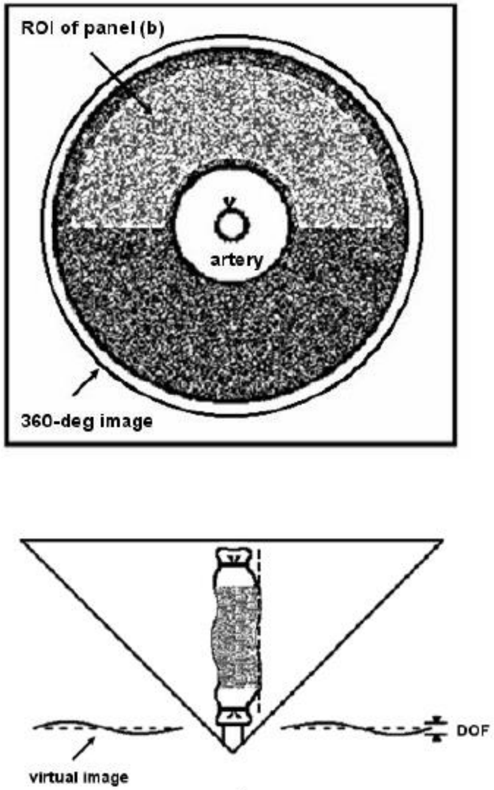

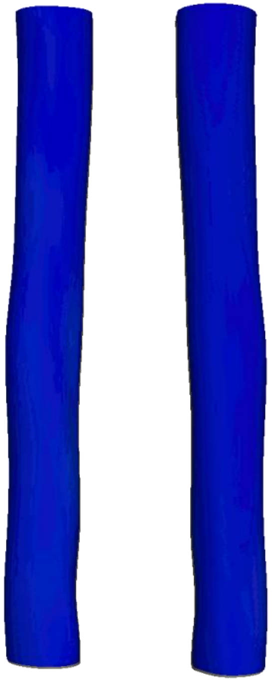

avril@emse.fr

pDIC measurements

Fibulin 4 SMC KO

6852

ventral *dorsal* *inflation*

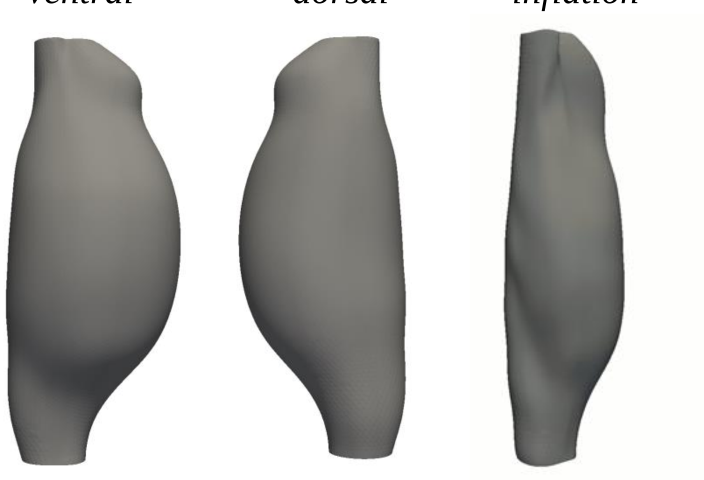

Fibrillin 1 *mgR/mgR*

CS38

ventral *dorsal* *inflation*

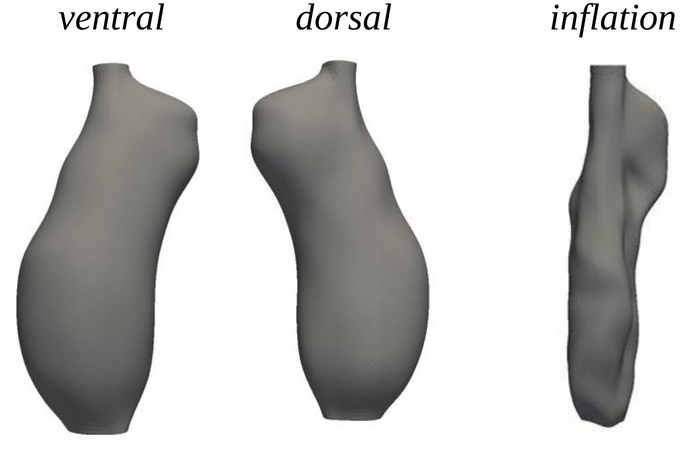

avril@emse.fr

Measurement of bulk deformation fields by Digital Volume Correlation on OCT images

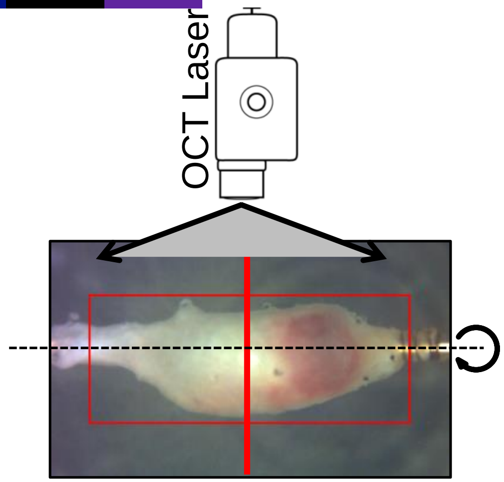

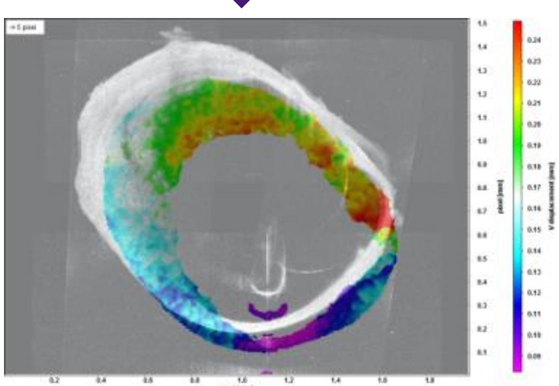

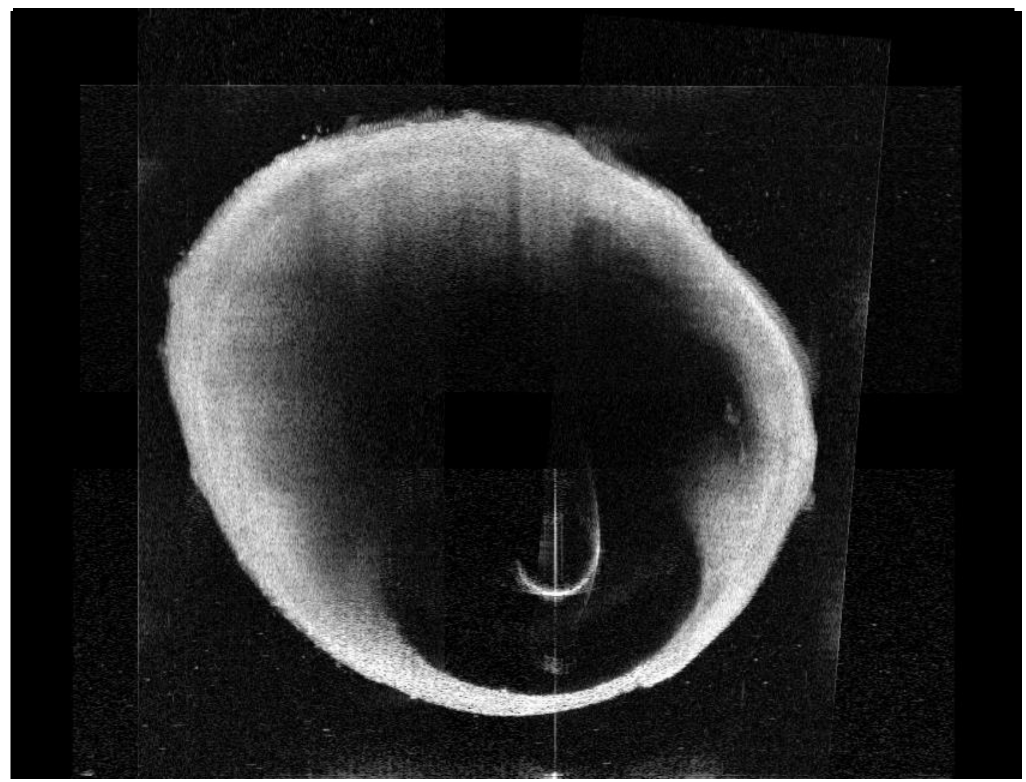

OCT-DVC applied to arterial mechanics

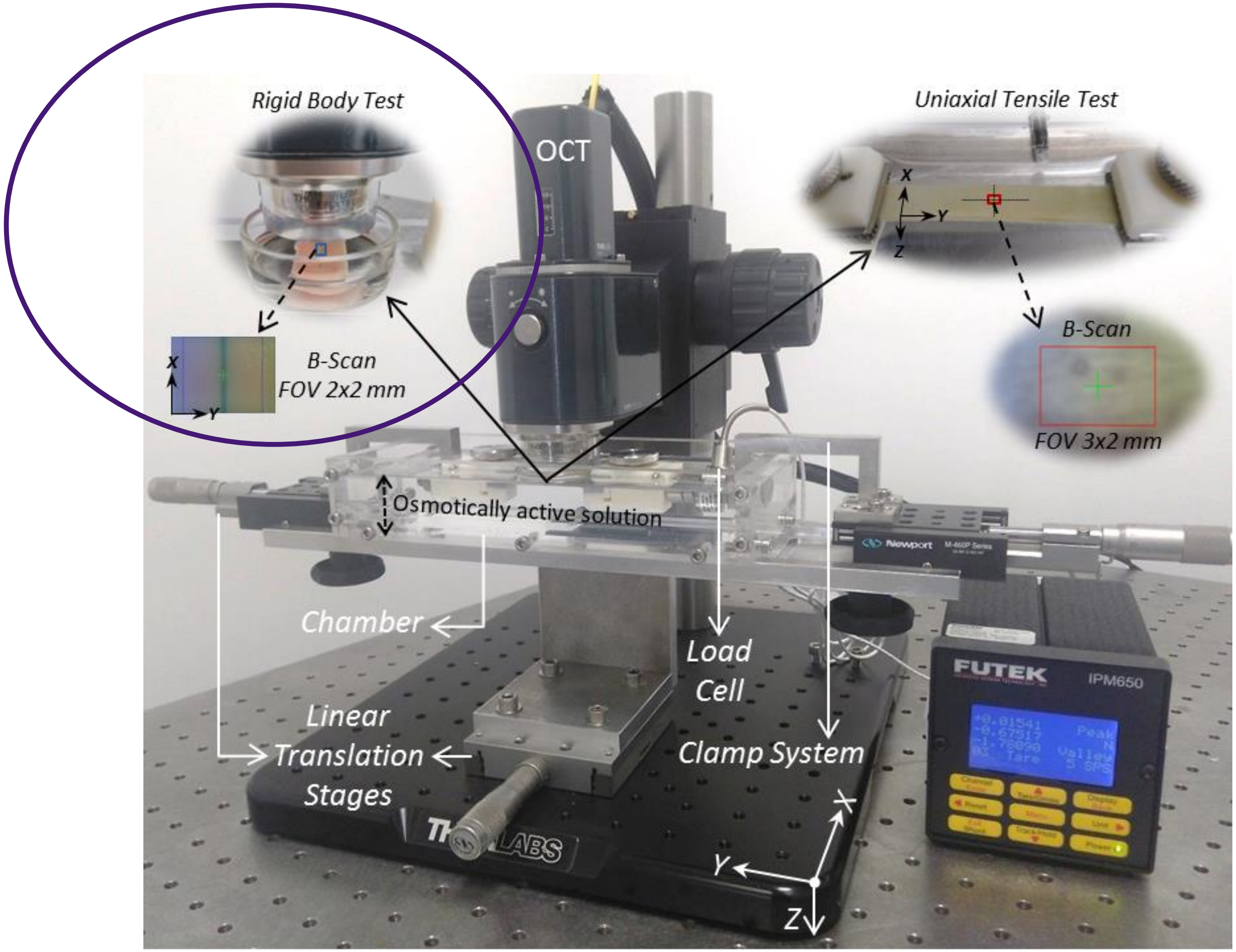

avril@emse.fr

MINES Saint-Étienne

OCT-DVC validation – Rigid Motion

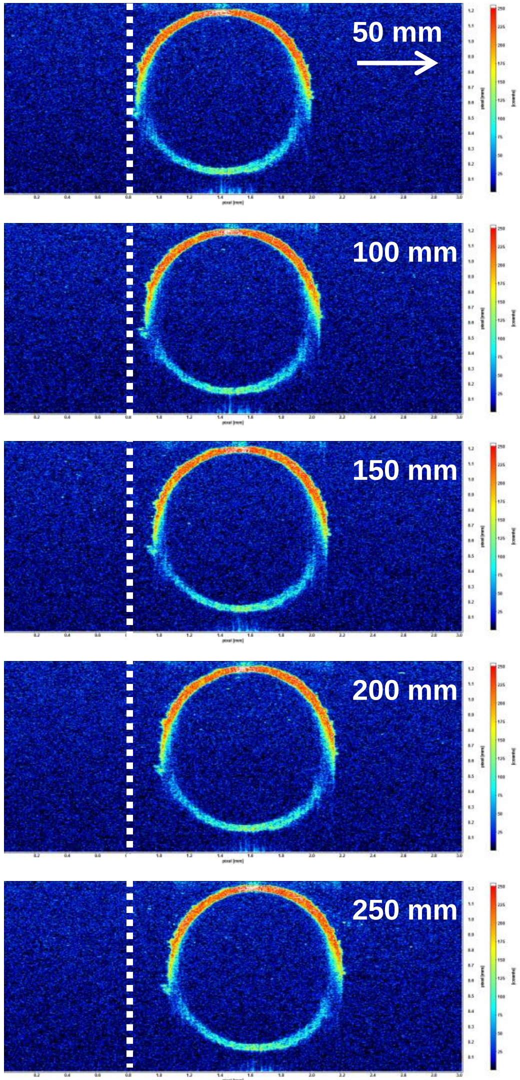

Digital Volume Correlation

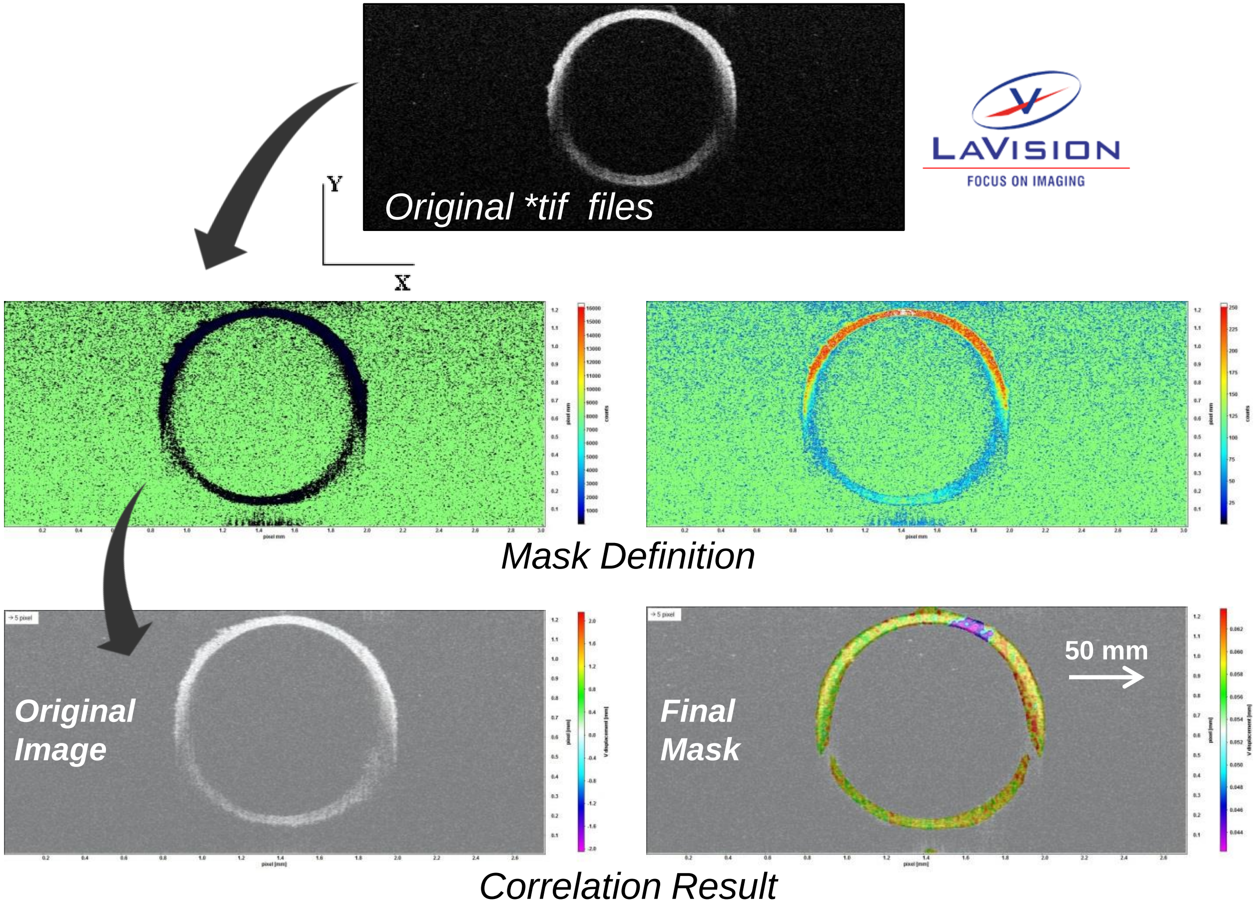

Rigid Motion Results
Strains (xx, yy, xy) - Displacements

Infinitesimal Strain
Green Strain

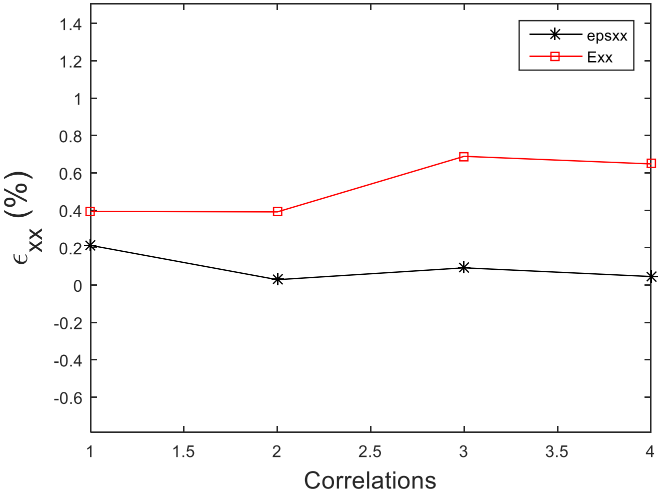

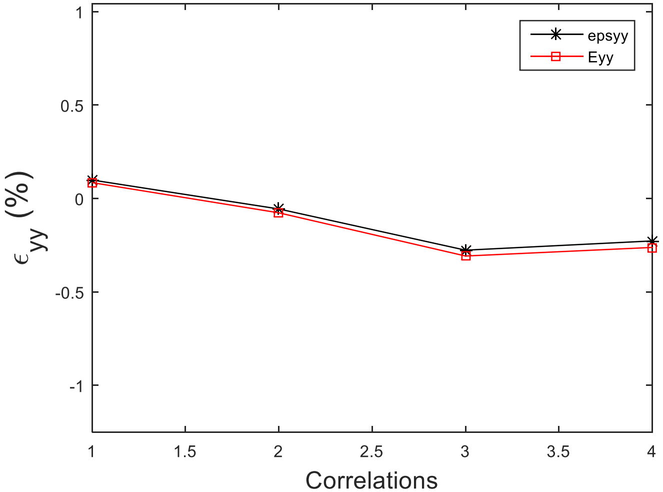

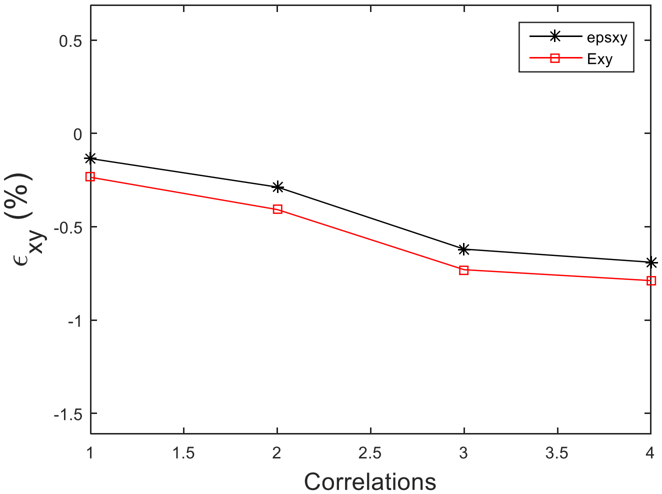

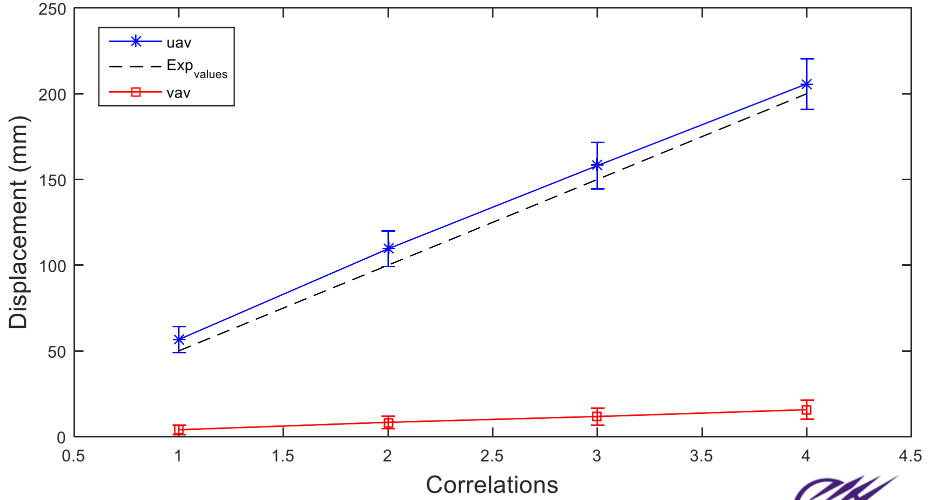

OCT-DVC applied to arterial mechanics

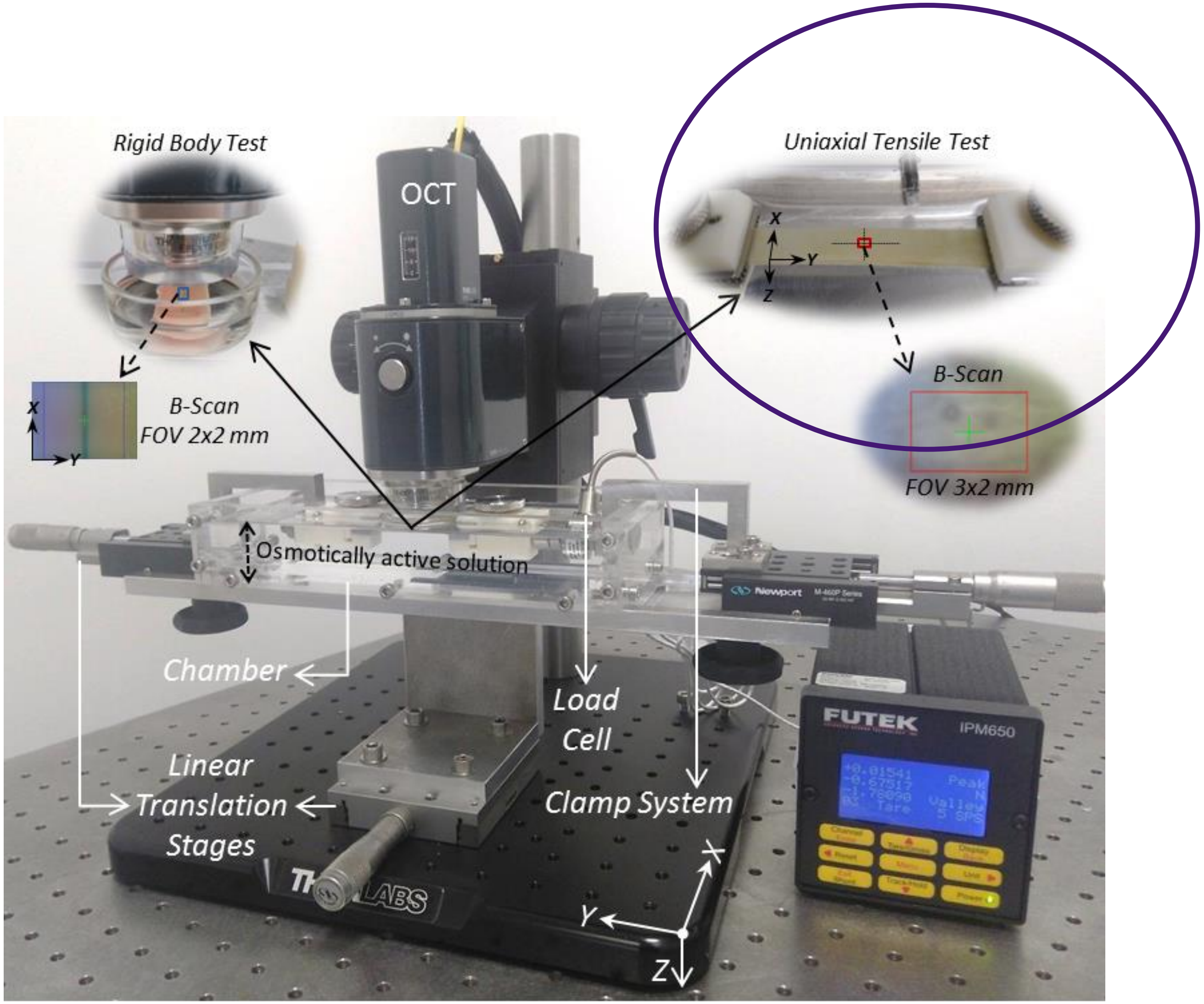

avril@emse.fr

MINES Saint-Étienne

OCT-DVC applied to arterial mechanics

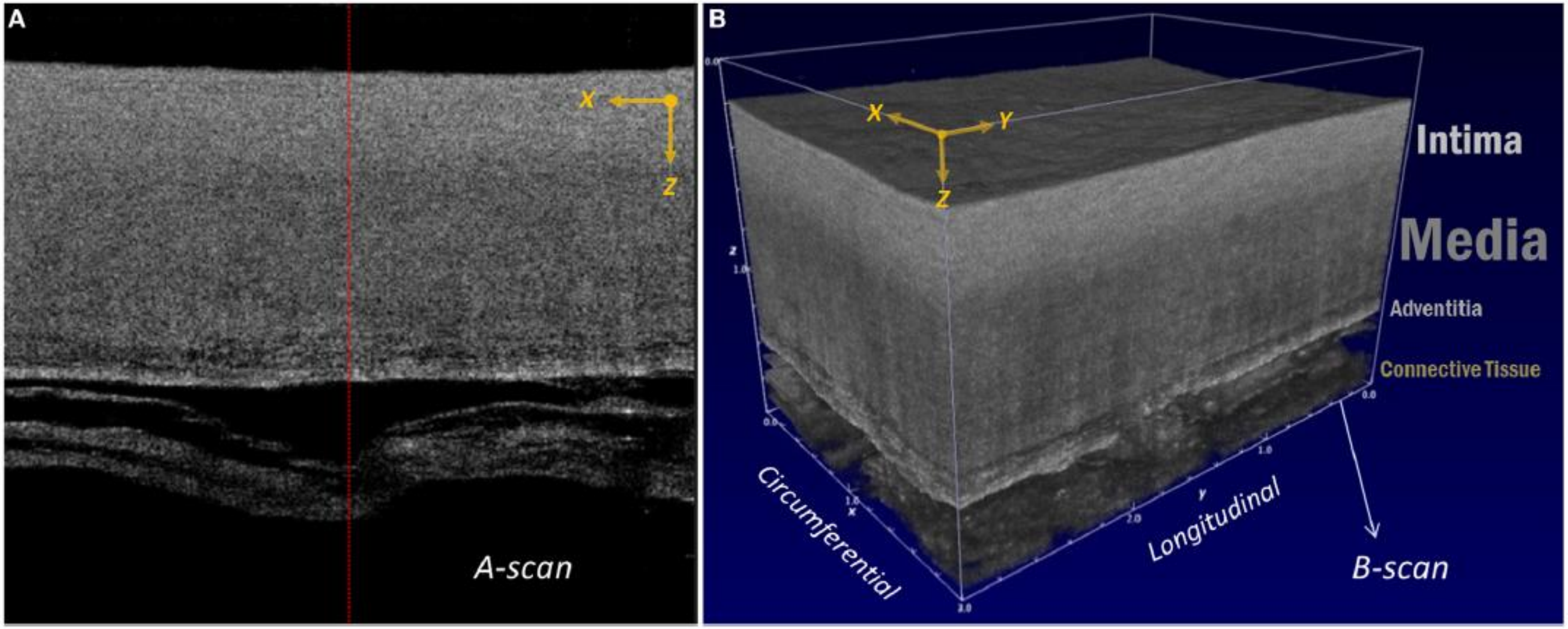

avril@emse.fr

OCT-DVC applied to arterial mechanics

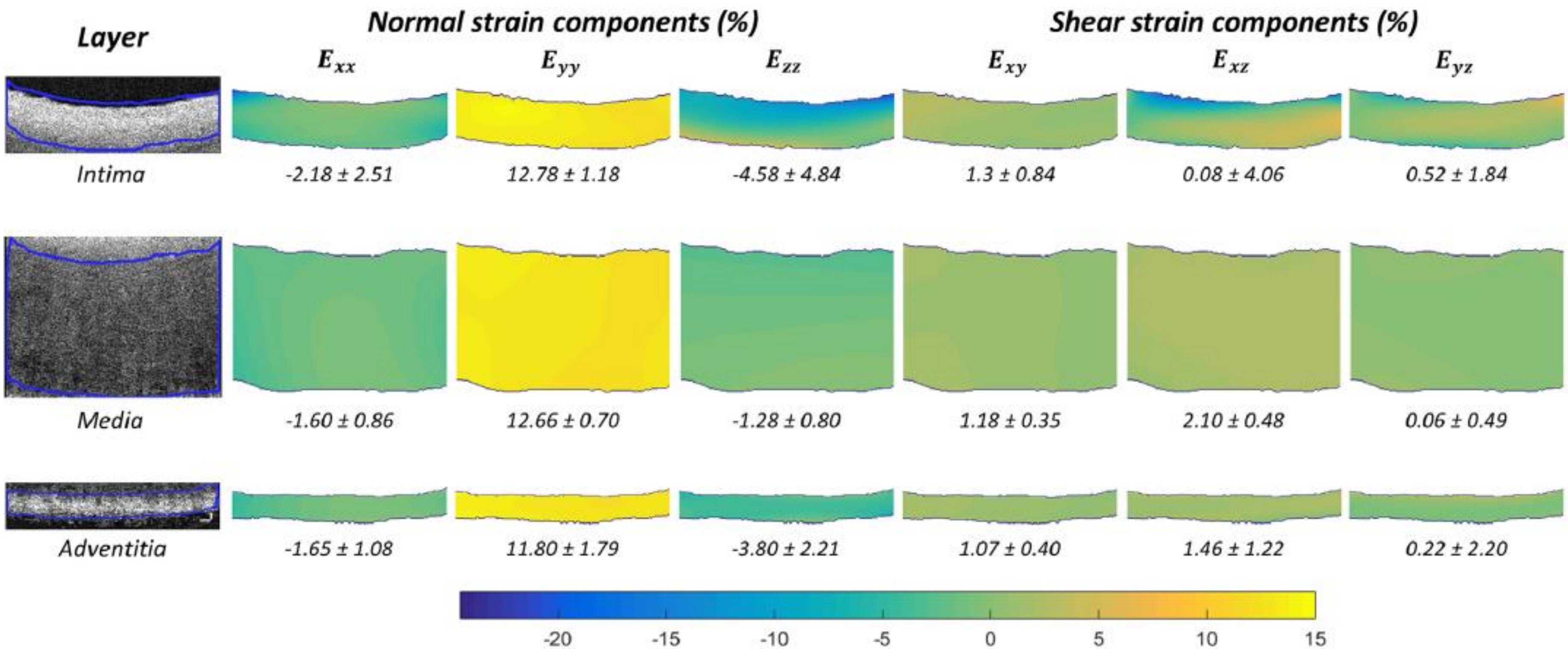

APPROACH

1. Experiments
2. **Material model**
3. Inverse method

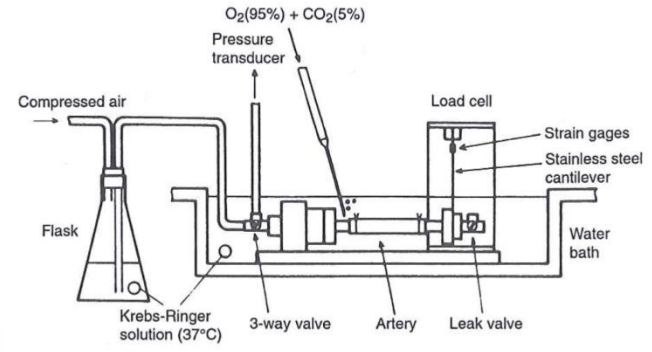

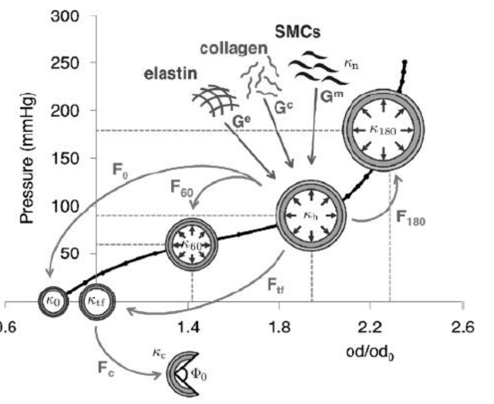

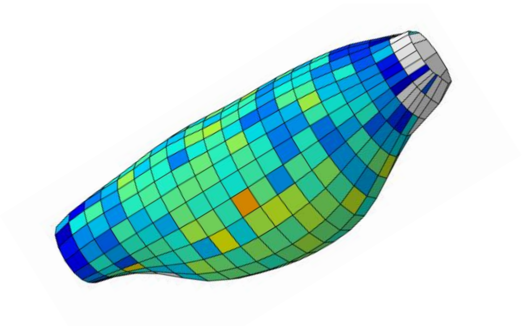

CONSTITUTIVE MODEL

Bellini, et al., Ann. Biomed. Eng., **42**(3), pp. 488–502, 2014

Strain energy functions:

$$W = \phi^{\mathrm{e}} W^{\mathrm{e}}(\mathbf{F}^{\mathrm{e}}) + \phi^{\mathrm{m}} W^{\mathrm{m}}(\lambda^{\mathrm{m}}) + \sum_{j=1}^{4} \phi^{\mathrm{c}_j} W^{\mathrm{c}_j}(\lambda^{\mathrm{c}_j})$$

$$W^{\mathrm{e}}(\mathbf{F}^{\mathrm{e}}) = \frac{c^{\mathrm{e}}}{2}\left[\mathrm{tr}\left((\mathbf{F}^{\mathrm{e}})^{\mathrm{T}}\mathbf{F}^{\mathrm{e}}\right) - 3\right]$$

$$W^{\mathrm{m}}(\lambda^{\mathrm{m}}) = \frac{c_2^{\mathrm{m}}}{4c_3^{\mathrm{m}}}\left[e^{c_3^{\mathrm{m}}\left((\lambda^{\mathrm{m}})^2-1\right)^2} - 1\right]$$

$$W^{\mathrm{c}}(\lambda^{\mathrm{c}_j}) = \frac{c_2^{\mathrm{c}}}{4c_3^{\mathrm{c}}}\left[e^{c_3^{\mathrm{c}}\left((\lambda^{\mathrm{c}_j})^2-1\right)^2} - 1\right]$$

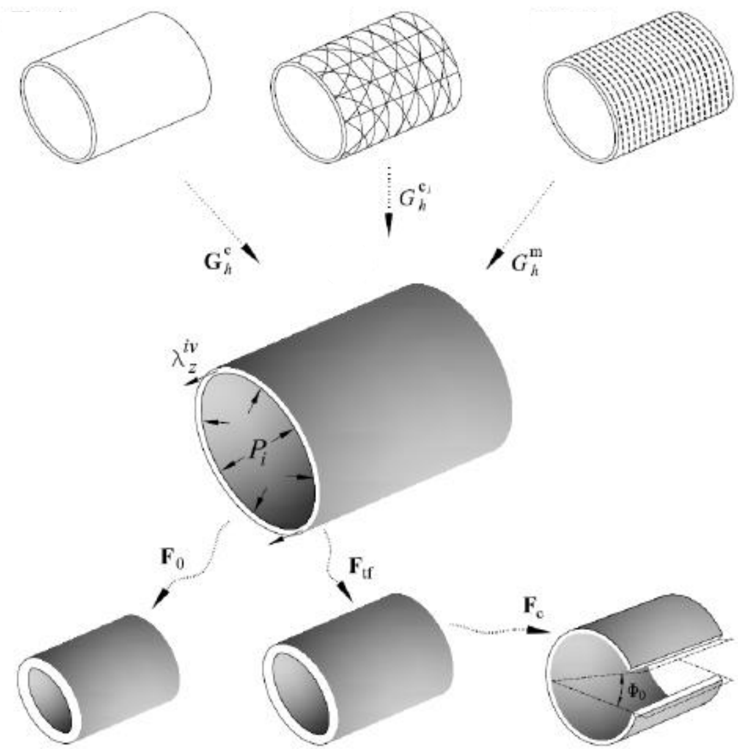

avril@emse.fr

MINES Saint-Étienne

CONSTITUTIVE MODEL

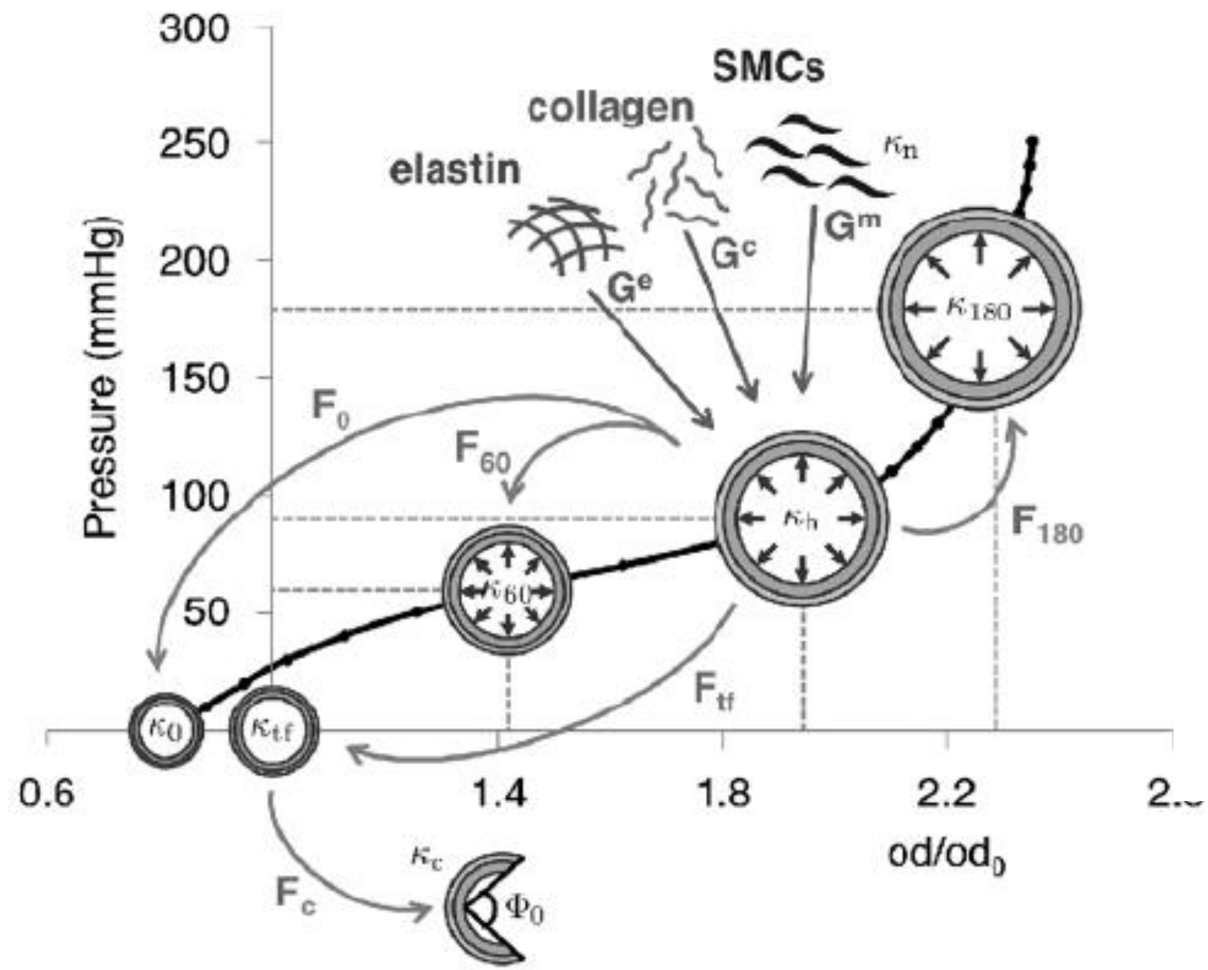

FE implementation

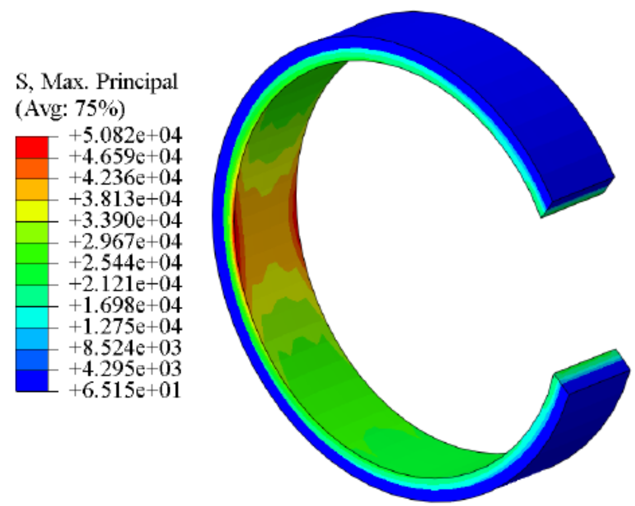

Bellini, et al., Ann. Biomed. Eng., **42**(3), pp. 488–502, 2014

MINES Saint-Étienne

PARAMETERS TO BE IDENTIFIED

$$W = \phi^{e} W^{e}(\mathbf{F}^{e}) + \phi^{m} W^{m}(\lambda^{m}) + \sum_{j=1}^{4} \phi^{c_j} W^{c_j}(\lambda^{c_j})$$

$$W^{e}(\mathbf{F}^{e}) = \frac{c^{e}}{2}\left[\mathrm{tr}\left((\mathbf{F}^{e})^{T}\mathbf{F}^{e}\right) - 3\right]$$

$$W^{m}(\lambda^{m}) = \frac{c_2^{m}}{4c_3^{m}}\left[e^{c_3^{m}((\lambda^{m})^2-1)^2} - 1\right]$$

$$W^{c}(\lambda^{c_j}) = \frac{c_2^{c}}{4c_3^{c}}\left[e^{c_3^{c}((\lambda^{c_j})^2-1)^2} - 1\right]$$

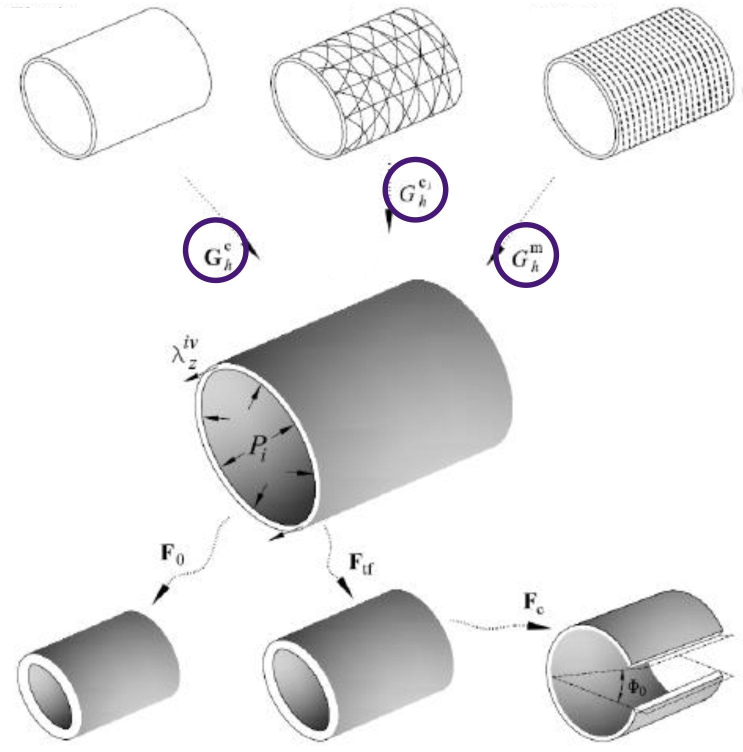

MINES Saint-Étienne

APPROACH

1. Experiments
2. Material model
3. **Inverse method**

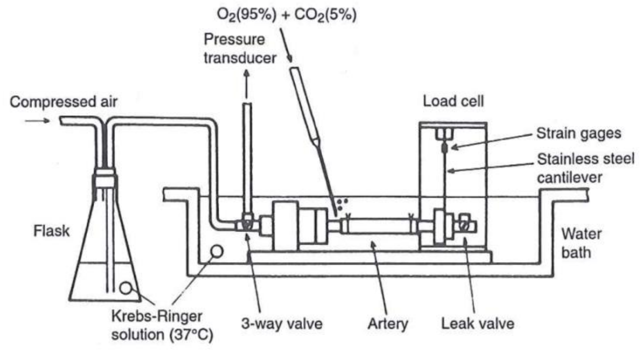

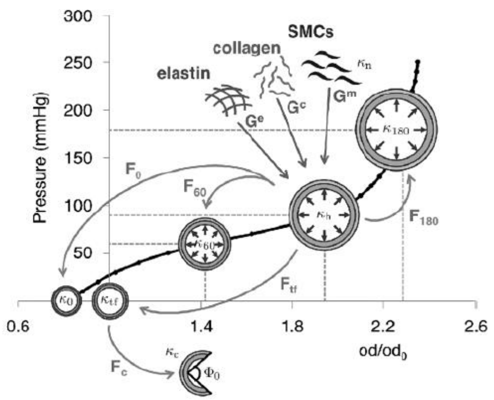

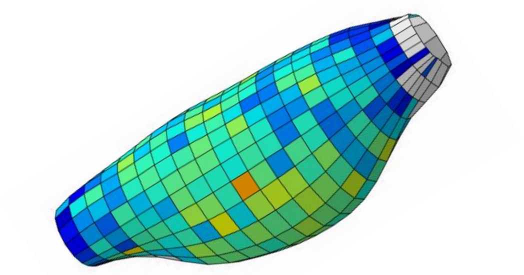

avril@emse.fr

MINES Saint-Étienne

Inverse approach – traditional approach

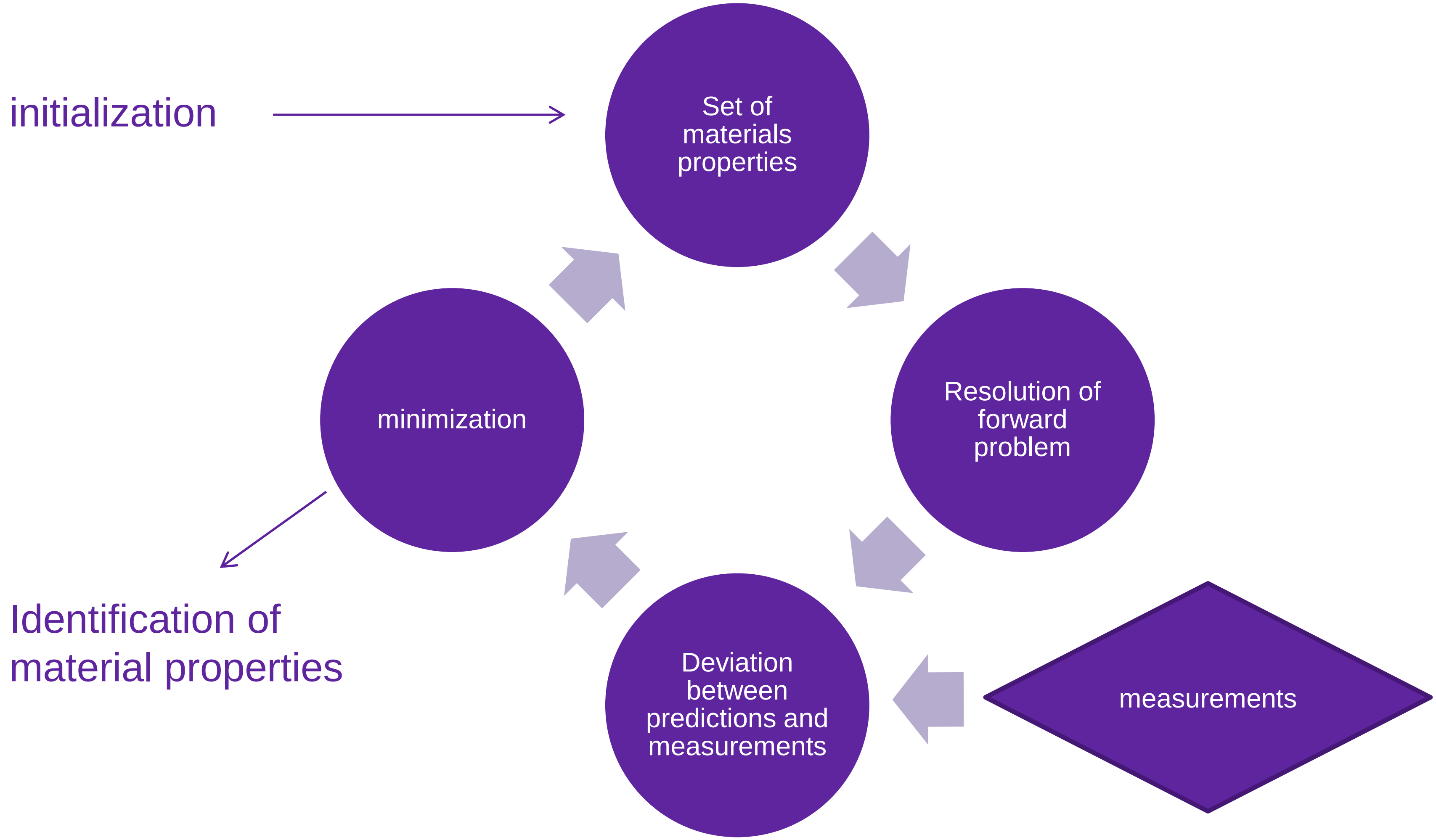

avril@emse.fr

MINES Saint-Étienne

Inverse approach – FEMU approach

initialization →

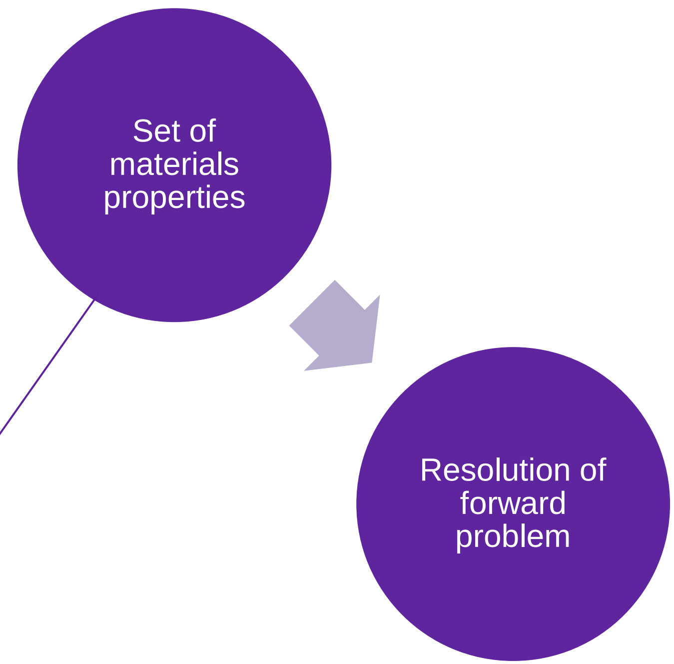

1. Write the weak form of the problem:

$$R(u, w, \mu) = 0 \quad \forall w$$

2. Discretize and represent as a linear combination of piecewise bilinear functions

$$u^h = \sum U_i \varphi_i(\mathbf{x})$$
$$w^h = \sum W_i \varphi_i(\mathbf{x})$$
$$\mu^h = \sum \mu_i \varphi_i(\mathbf{x})$$

3. Implement a finite-element implicit resolution using the BFGS algorithm

avril@emse.fr

MINES Saint-Étienne

Inverse approach – FEMU approach

initialization →

Set of materials properties

Oberai et al., Inverse problems, **19**, pp. 297-313, 2003

Resolution of forward problem

Deviation between predictions and measurements

measurements

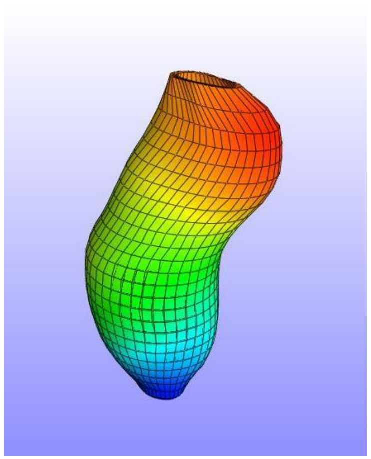

$$J(\mu) = \|T(u) - T(u^{exp})\|^2 + \frac{\alpha}{2} B(\mu)$$

avril@emse.fr

Inverse approach – FEMU approach

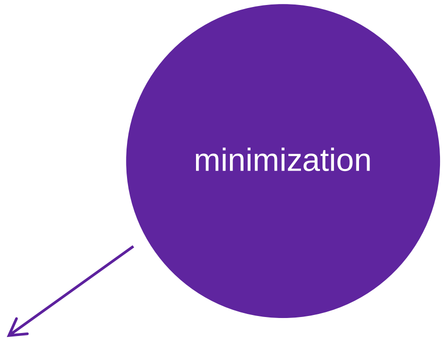

Identification of material properties

1. Use a gradient based method (steepest descent or BFGS)
2. Need to derive the gradient of J with respect to μ at each iteration. With the adjoint method, this requires the resolution of 2 forward problems
3. Very unstable with hyperelastic models: **many risks that the forward problems have a poor convergence**

avril@emse.fr

Alternative inverse approach: the virtual fields method

initialization

Identification of material properties

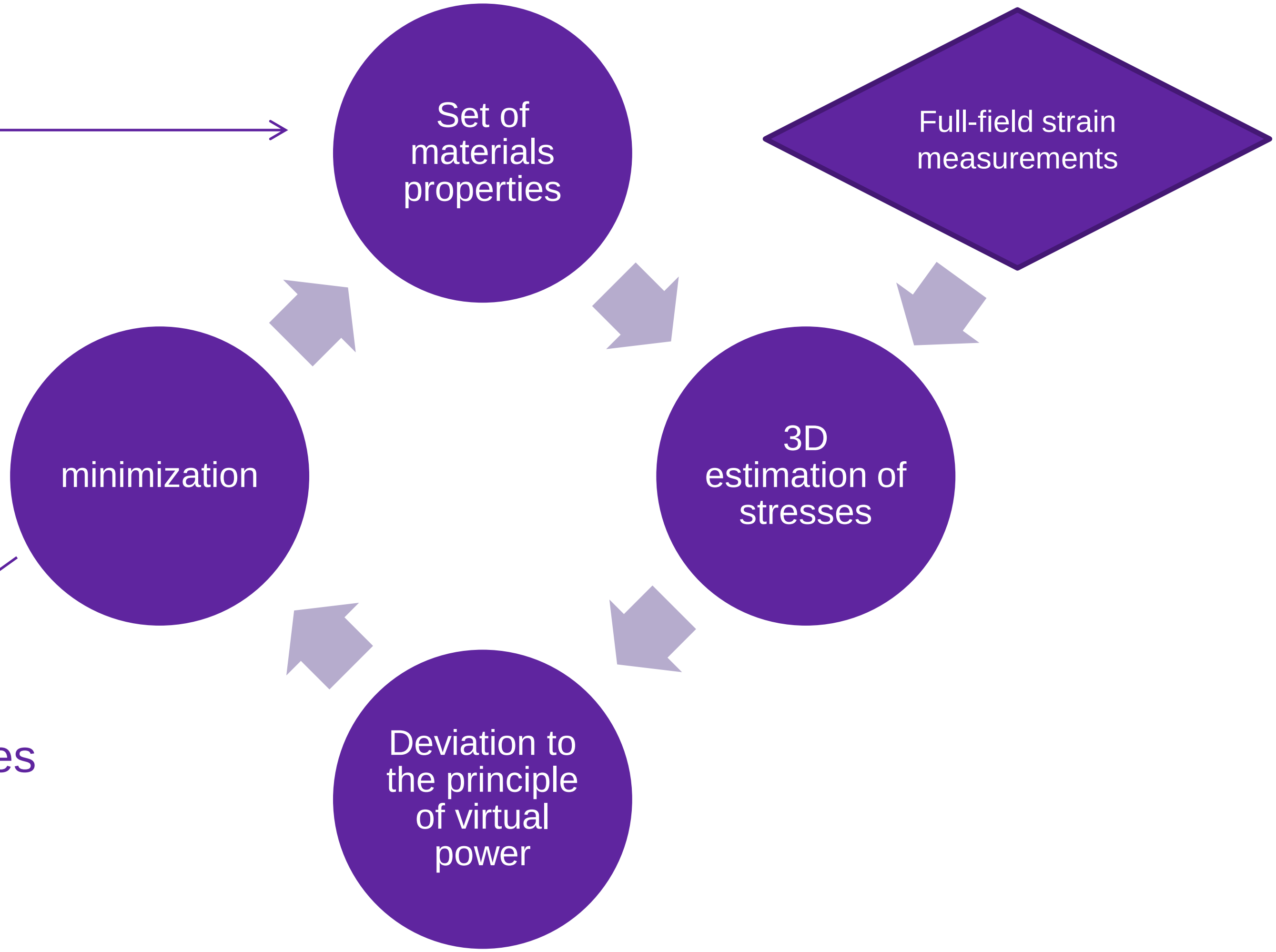

Bersi et al., J Biomech Eng, 2016

Full-field stress reconstruction

initialization →

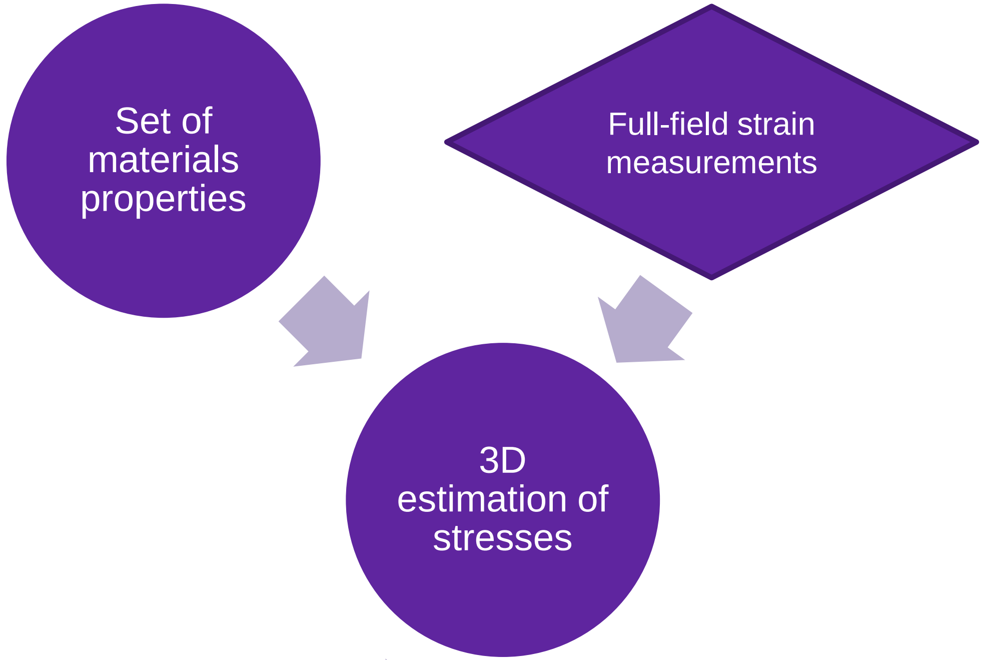

$$W = \phi^{e} W^{e}(\mathbf{F}^{e}) + \phi^{m} W^{m}(\lambda^{m}) + \sum_{j=1}^{4} \phi^{c_j} W^{c_j}(\lambda^{c_j})$$

$$W^{e}(\mathbf{F}^{e}) = \frac{c^{e}}{2}\left[\mathrm{tr}\left((\mathbf{F}^{e})^{T}\mathbf{F}^{e}\right) - 3\right]$$

$$W^{m}(\lambda^{m}) = \frac{c_2^{m}}{4c_3^{m}}\left[e^{c_3^{m}\left((\lambda^{m})^2-1\right)^2} - 1\right]$$

$$W^{c}(\lambda^{c_j}) = \frac{c_2^{c}}{4c_3^{c}}\left[e^{c_3^{c}\left((\lambda^{c_j})^2-1\right)^2} - 1\right]$$

Simple application of the constitutive model for each element

Minimization of the equilibrium gap using the principle of virtual power

minimization

$$J = \sum_{p}\sum_{\lambda}\left(\underbrace{-\int_{\omega(t)}\underline{\underline{\sigma}}:\left(\underline{\nabla}\otimes\underline{\xi}^{*}\right)d\omega}_{P^{*}_{int}} + \underbrace{\oint_{\partial\omega(t)}\underline{T}:\underline{\xi}^{*}\,ds}_{P^{*}_{ext}}\right)^{2}$$

Bersi et al., J Biomech Eng, 2016

Resolution:

$$\min_{c_3^1, c_3^{2,3}, c_3^4, \alpha, \beta}\left[\min_{c^e, c_2^1, c_2^{2,3}, c_2^4}\left[\frac{J(u)}{A}+\frac{J(v)}{B}\right]\right]$$

Linear least-squares (inner minimization)

Genetic algorithm (outer minimization)

avril@emse.fr

How to obtain 3D full-field strain measurements?

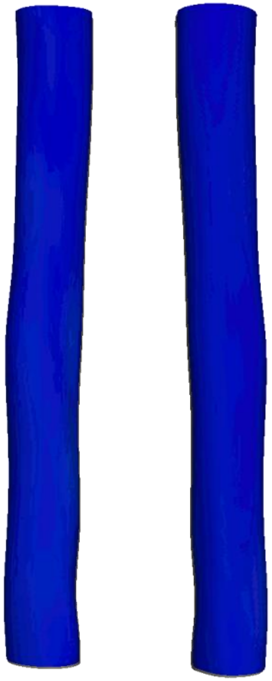

Posterior Anterior

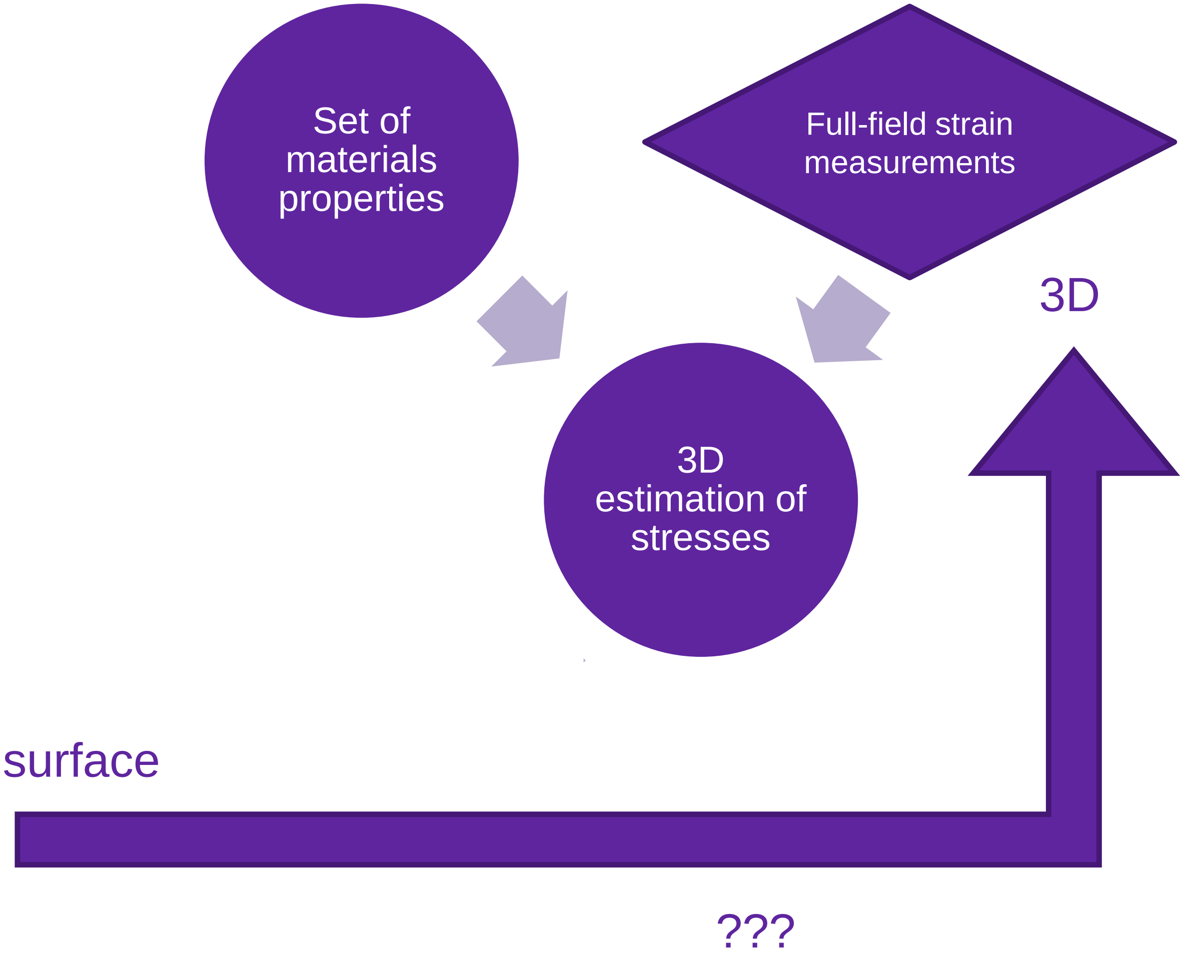

Measurement of bulk deformation fields by Digital Volume Correlation on OCT images

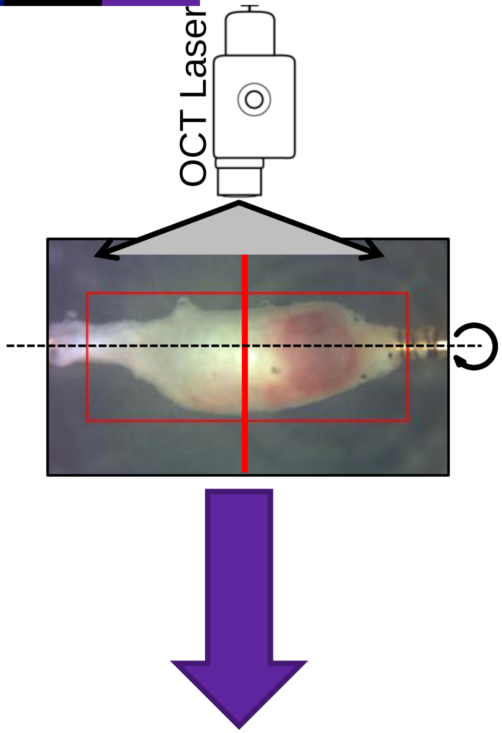

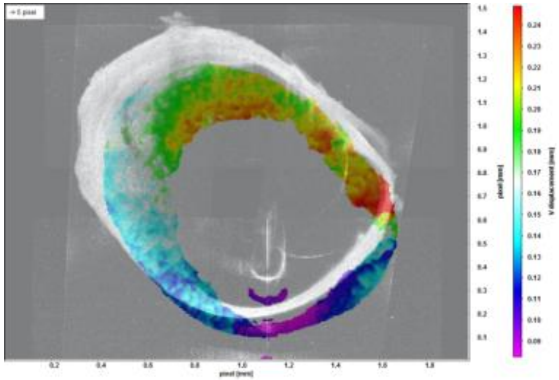

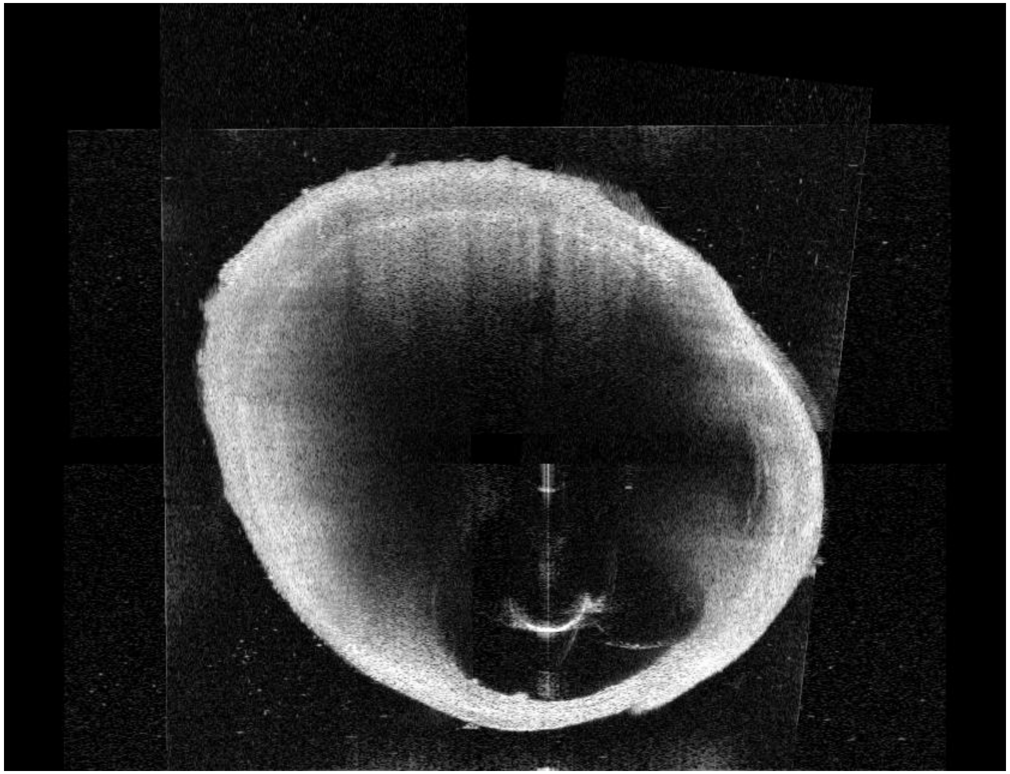

avril@emse.fr

Derivation of stress tensor using layer specific constitutive behavior

3D estimation of strains

3D estimation of stress

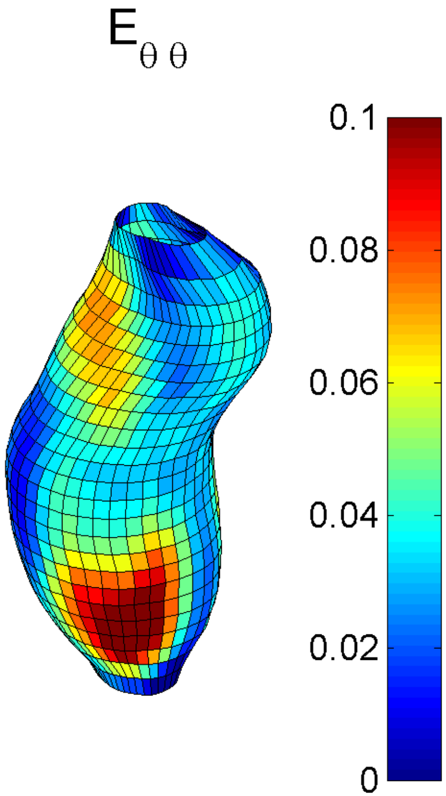

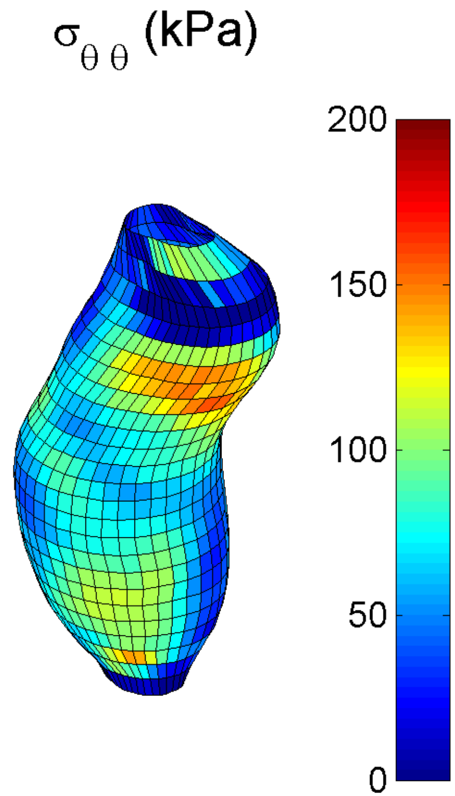

avril@emse.fr

MINES Saint-Étienne

Minimizing the equilibrium gap

minimization

$$J = \sum_{p} \sum_{\lambda} \left(\underbrace{-\int_{\omega(t)} \underline{\underline{\sigma}} : \left(\underline{\nabla} \otimes \underline{\xi}^{*} \right) d\omega}_{P_{int}^{*}} + \underbrace{\oint_{\partial\omega(t)} \underline{T} : \underline{\xi}^{*} \, ds}_{P_{ext}^{*}} \right)^{2}$$

Bersi et al., J Biomech Eng, 2016

Resolution:

$$\min_{c_3^1, c_3^{2,3}, c_3^4, \alpha, \beta} \left[\min_{c^e, c_2^1, c_2^{2,3}, c_2^4} \left[\frac{J(u)}{A} + \frac{J(v)}{B} \right] \right]$$

Linear least-squares

Genetic algorithm

avril@emse.fr

Similar to material fitting at every position

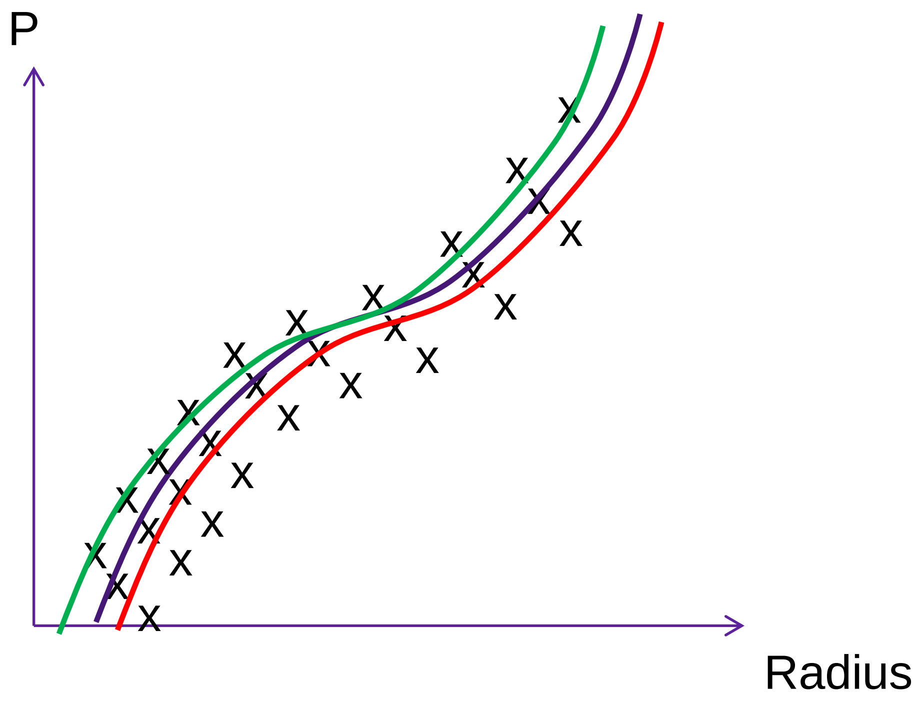

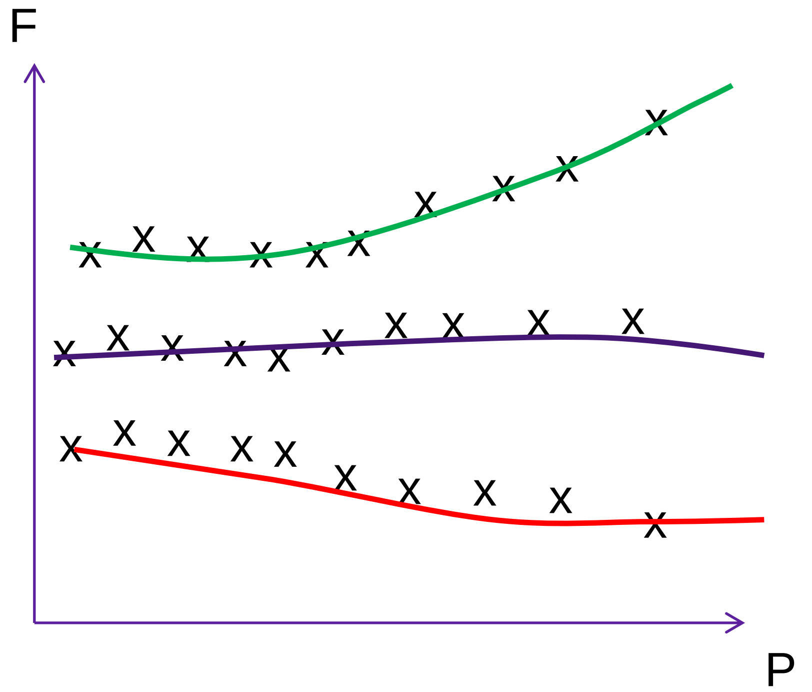

Crosses represent external virtual work for every pressure and axial stretch
Solid lines represent internal virtual work
The goodness of fit is evaluated with the R^2 value

Summary of the inverse approach

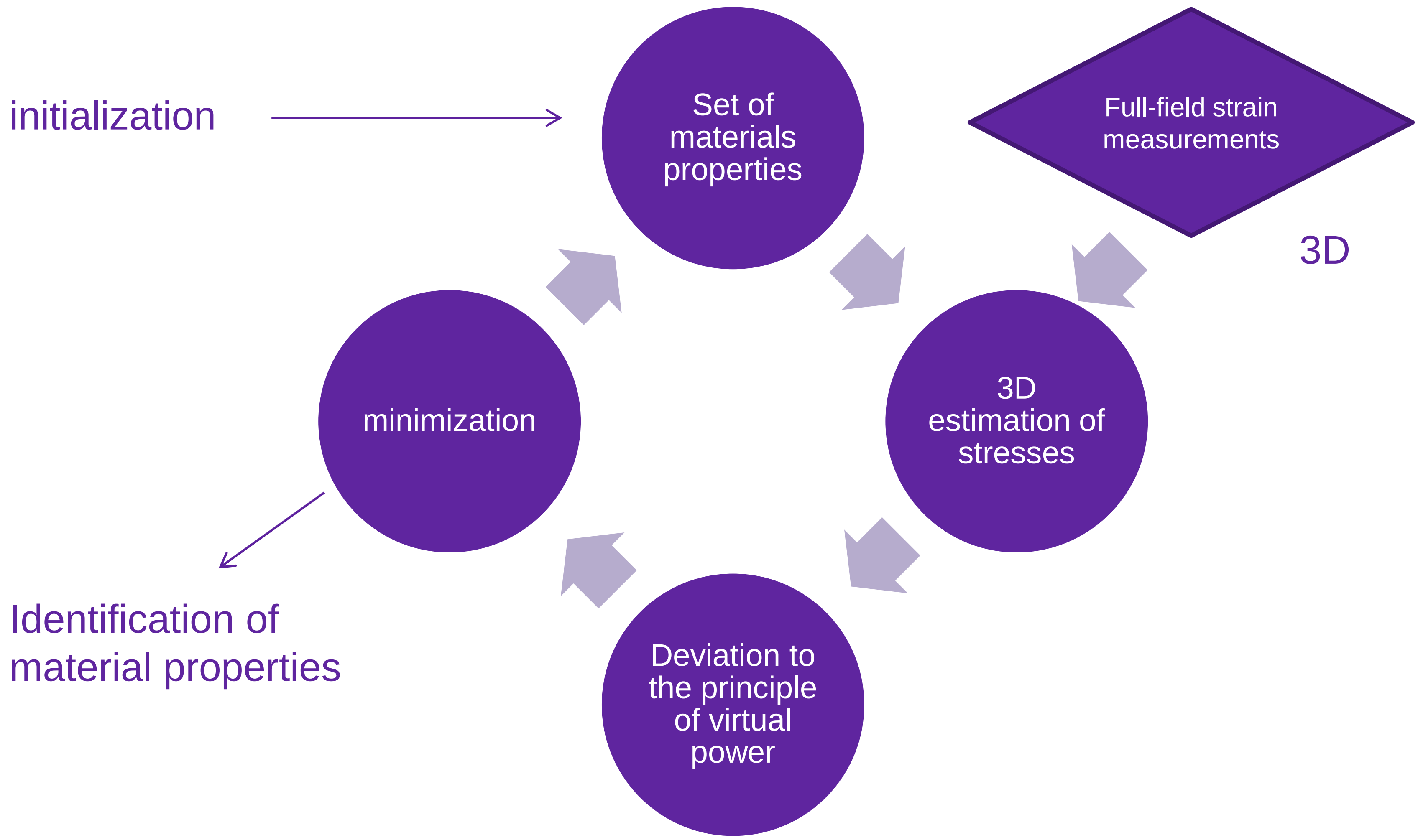

avril@emse.fr

Results - Highlights

avril@emse.fr

Full-Field Material Parameter Estimation vs thickness distribution

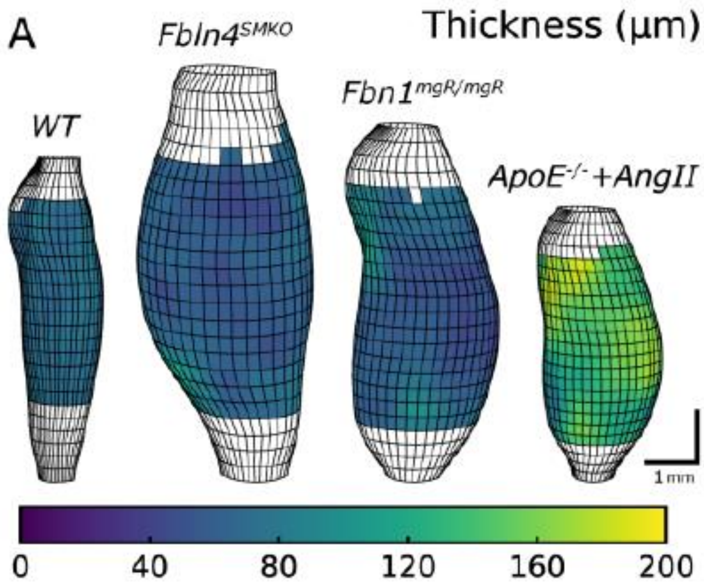

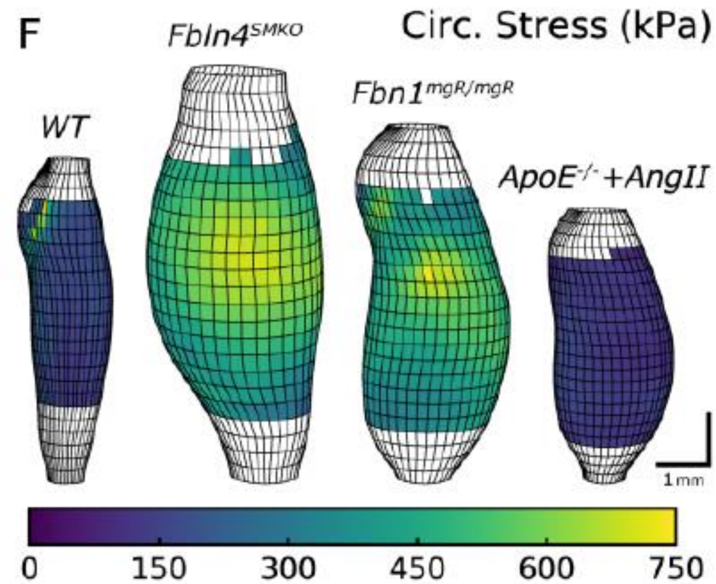

avril@emse.fr

Full-Field Material Parameter Estimation vs local stress

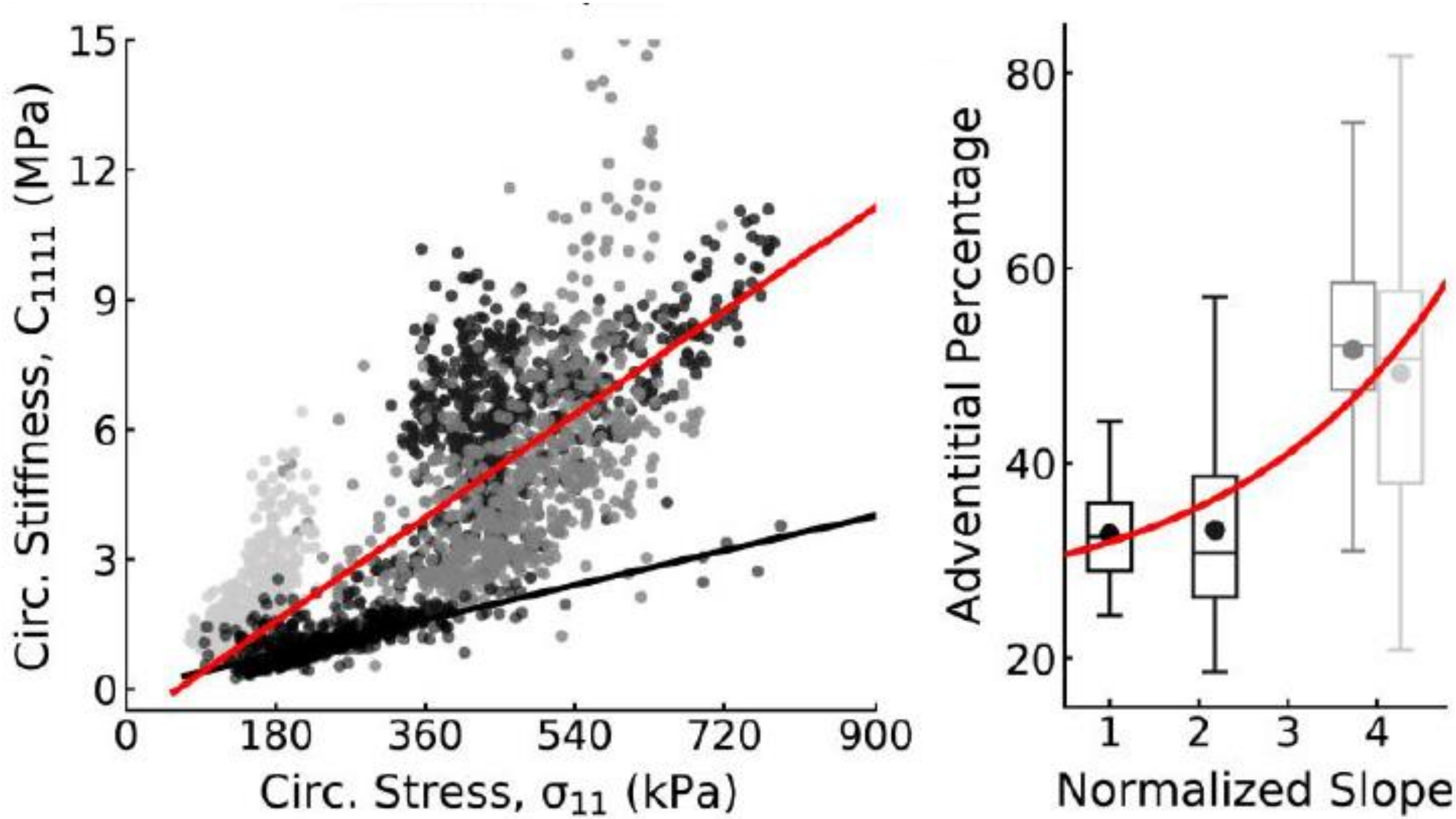

avril@emse.fr

MINES Saint-Étienne

Correlation with tissue µstructure

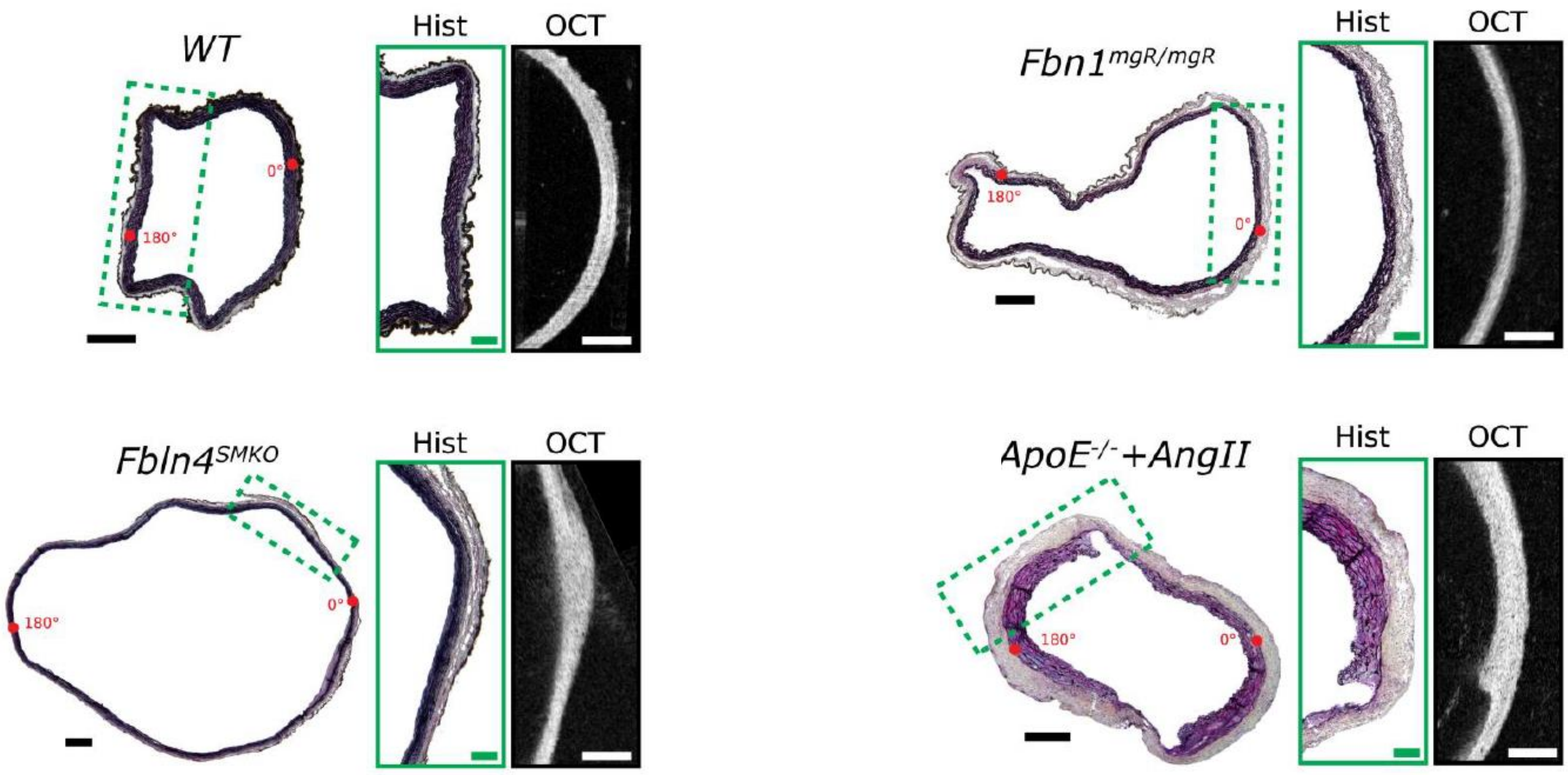

avril@emse.fr

Vision

- **Our vision is that the evolution of the strength and of the wall stress of the aorta during the growth of an aneurysm can be predicted on a patient-specific basis by a <u>computational model</u>.**

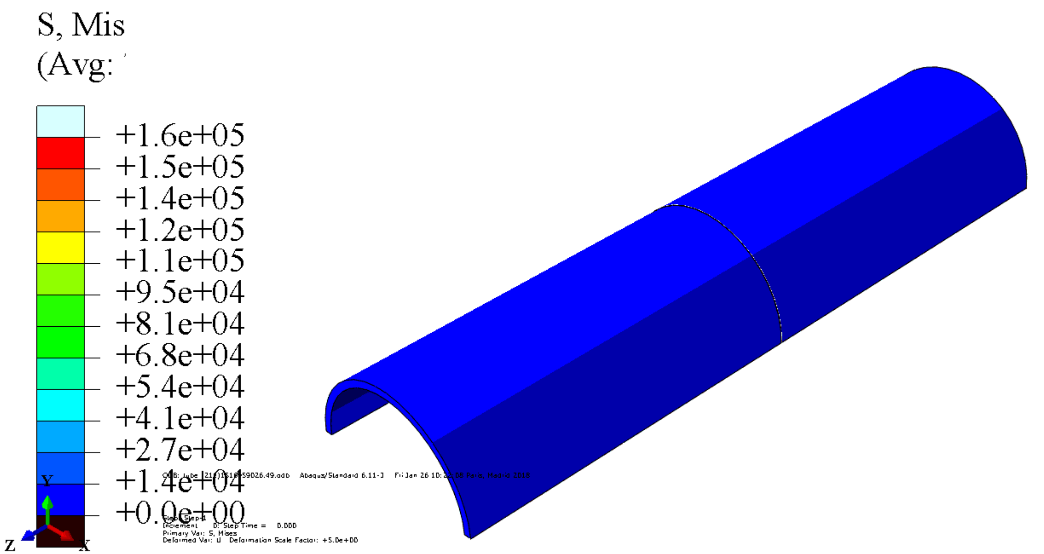

Joan Laubrie

avril@emse.fr

MINES Saint-Étienne

Some other projects in vascular mechanobiology

Non invasive reconstruction of in vivo stiffness distribution

Gated CT scan

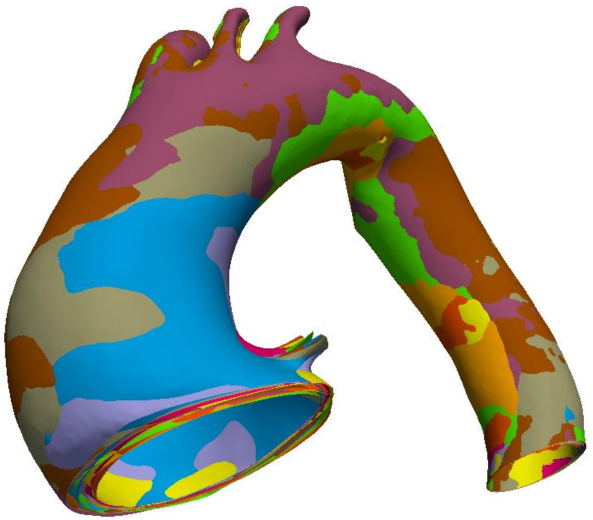

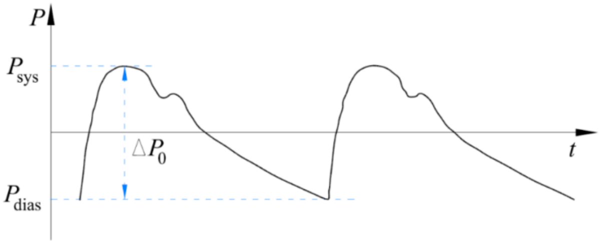

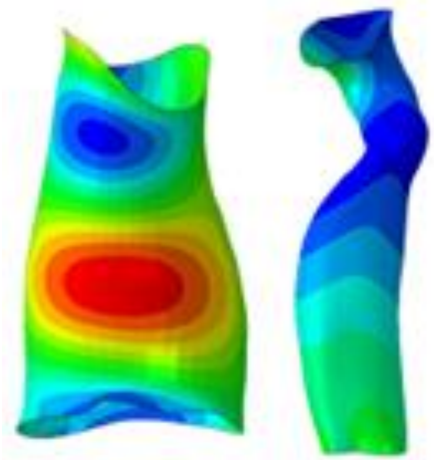

Stiffness map

Correlation with flow descriptors

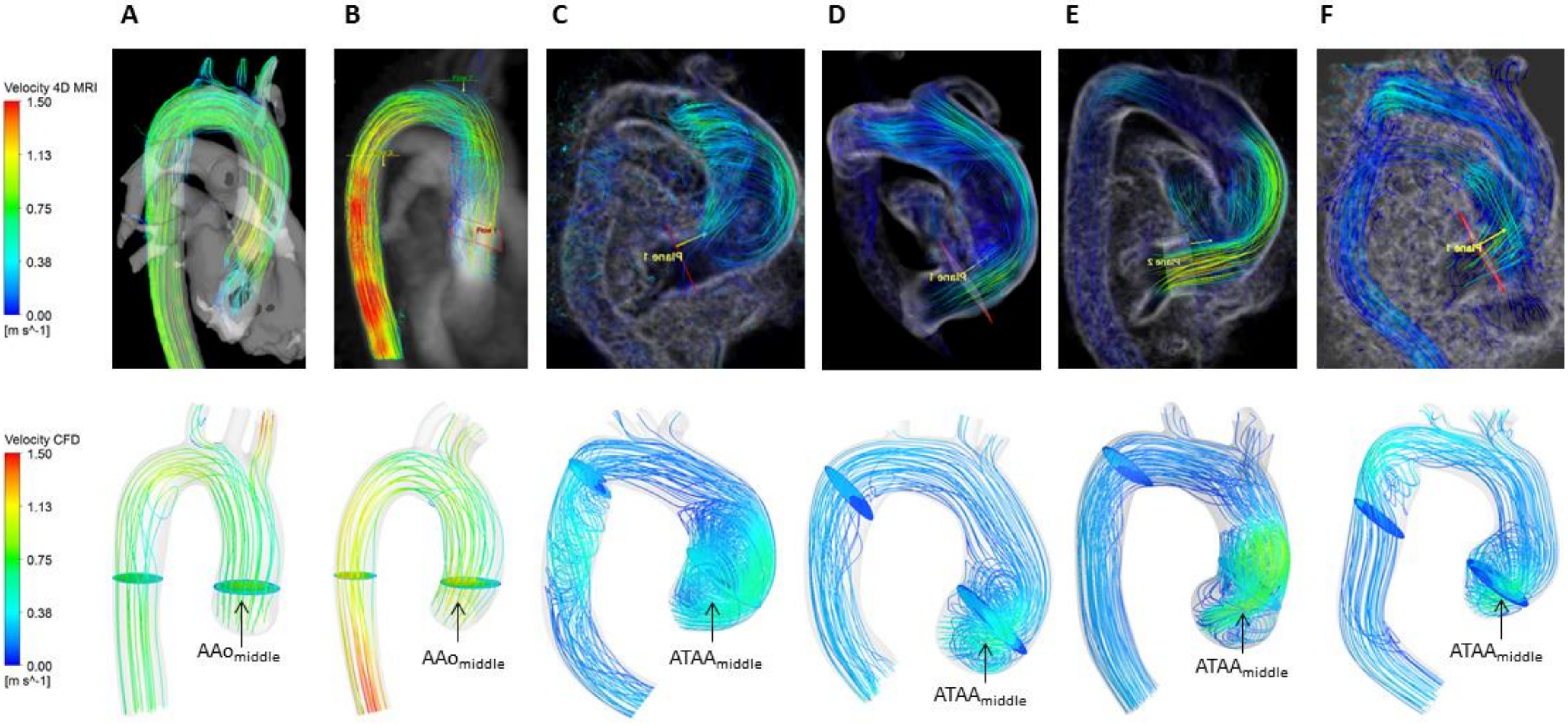

avril@emse.fr

MINES Saint-Étienne

Traction force microscopy of vascular smooth muscle cells

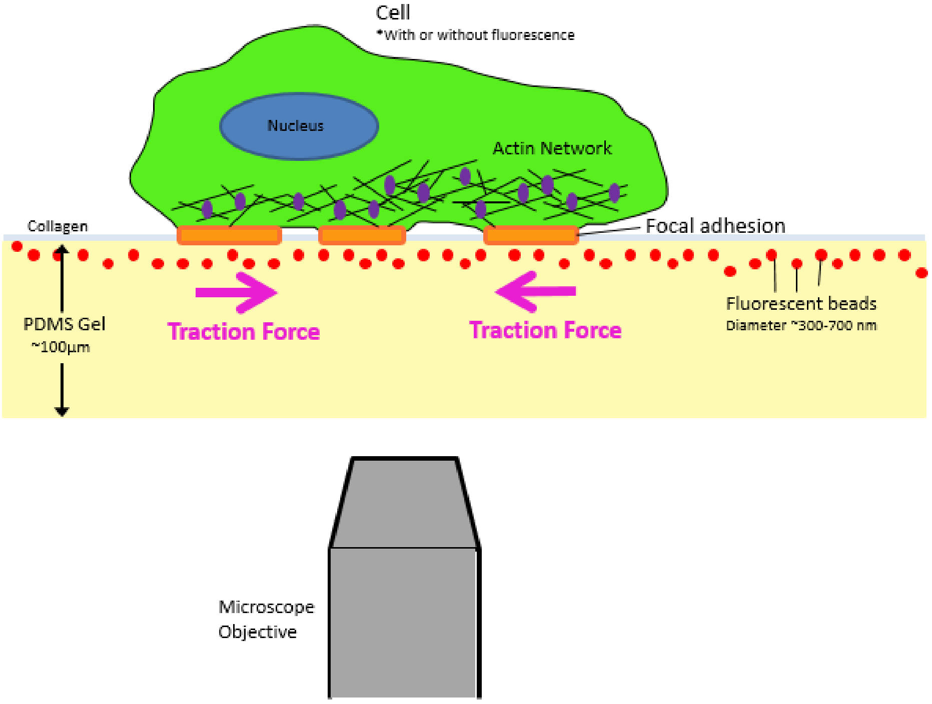

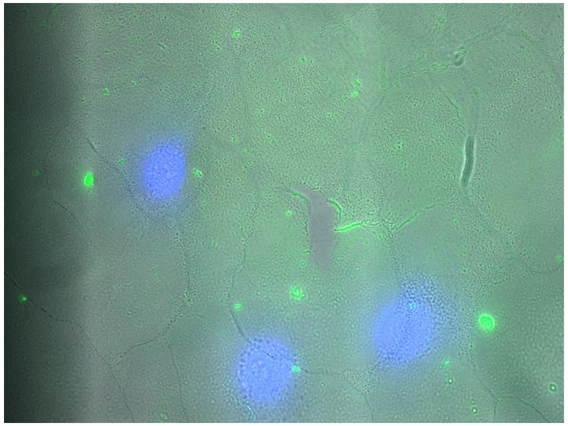

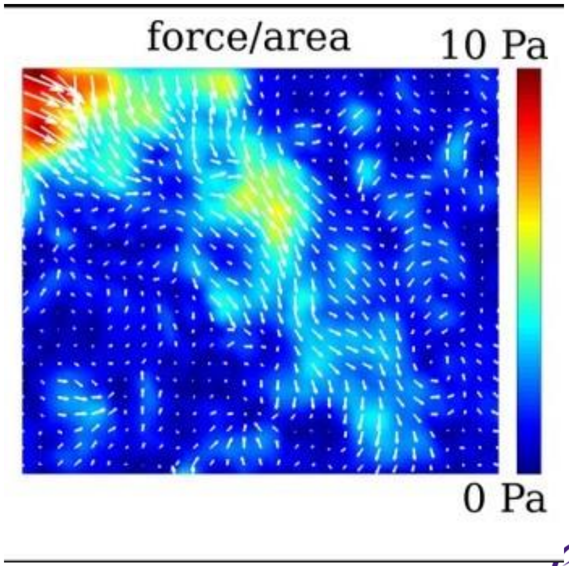

Acknowledgements

- Olfa Trabelsi
- Aaron Romo
- Jin Kim
- Pierre Badel
- Frances Davis
- Victor Acosta
- Jamal Mousavi
- Solmaz Farzeneh
- Francesca Condemi
- Cristina Cavinato
- Jérôme Molimard
- Baptiste Pierrat
- Joan Laubrie
- Claudie Petit

- Ambroise Duprey
- Jean-Pierre Favre
- Jean-Noël Albertini
- Salvatore Campisi
- Magalie Viallon
- Pierre Croisille

- Chiara Bellini
- Matthew Bersi
- Jay Humphrey
- Katia Genovese

Funding:
ERC-2014-CoG BIOLOCHANICS